Sedimentary Geology 219 (2009) 280–301

Contents lists available at ScienceDirect

Sedimentary Geology

journal homepage: www.elsevier.com/locate/sedgeo

Sequence stratigraphy and architecture of a late Early–Middle Aptian carbonate platform succession from the western Maestrat Basin (Iberian Chain, Spain)

Telm Bover-Arnal [a,*], Ramon Salas [b], Josep A. Moreno-Bedmar [b], Klaus Bitzer [a]

[a] Abteilung Geologie, Fakultät für Biologie, Chemie und Geowissenschaften, Universität Bayreuth, Universitätsstr, 30, 95440, Bayreuth, Germany
[b] Departament de Geoquímica, Petrologia i Prospecció Geològica, Facultat de Geologia, Universitat de Barcelona, Martí i Franqués s/n, 08028, Barcelona, Spain

ARTICLE INFO

Article history:
Received 1 December 2008
Received in revised form 7 May 2009
Accepted 15 May 2009

Keywords:
Sequence stratigraphy
Carbonate platforms
Sea-level changes
Aptian
Iberian Chain
Spain

ABSTRACT

The attributes of a 'four-systems-tract' sequence are at times difficult to identify in outcrop-scale carbonate successions. Poor exposure conditions, variable rates of sediment production, erosion and/or superposition of surfaces that are intrinsic to the nature of carbonate systems frequently conceal or remove its physical features. The late Early–Middle Aptian platform carbonates of the western Maestrat Basin (Iberian Chain, Spain) display facies heterogeneity enabling platform, platform-margin and slope geometries to be identified, and provide a case study that shows all the characteristics of a quintessential four systems tract-based sequence. Five differentiated systems tracts belonging to two distinct depositional sequences can be recognized: the Highstand Systems Tract (HST) and Forced Regressive Wedge Systems Tract (FRWST) of Depositional Sequence A; and the Lowstand Prograding Wedge Systems Tract (LPWST), Transgressive Systems Tract (TST) and subsequent return to a highstand stage of sea-level (HST) of Depositional Sequence B. An extensive carbonate platform of rudists and corals stacked in a prograding pattern marks the first HST. The FRWST is constituted by a detached, slightly cross-bedded calcarenite situated at the toe of the slope in a basinal position. The LPWST is characterized by a small carbonate platform of rudists and corals downlapping over the FRWST and onlapping landwards. The TST exhibits platform backstepping and marly sedimentation. Resumed carbonate production in shelf and slope settings characterizes the second HST. A basal surface of forced regression, a subaerial unconformity, a correlative conformity, a transgressive surface and a maximum flooding surface bound these systems tracts, and are well documented and widely mappable across the platform-to-basin transition area analyzed. Moreover, the sedimentary succession studied is made up of four types of parasequence that constitute stratigraphic units deposited within a higher-frequency sea-level cyclicity. Ten lithofacies associations form these basic accretional units. Each facies assemblage can be ascribed to an inferred depositional environment in terms of bathymetry, hydrodynamic conditions and trophic level. The architecture of the carbonate platform systems reflects a flat-topped non-rimmed depositional profile. Furthermore, these carbonate shelves are interpreted as having been formed in low hydrodynamic conditions. The long-term relative fall in sea-level occurred during the uppermost Early Aptian, which subaerially exposed the carbonate platform established during the first HST and resulted in the deposition of the FRWST, is interpreted as one of global significance. Moreover, a possible relationship between this widespread sea-level drop and glacio-eustasy seems plausible, and could be linked to the cooling event proposed in the literature for the late Early Aptian. Because of the important implications in sequence stratigraphy of this study, the sedimentary succession analyzed herein could serve as an analogue for the application of the four-systems-tract sequence stratigraphic methodology to carbonate systems.

1. Introduction

During the Aptian stage, the Tethyan realm underwent one of the most widespread developments of carbonate platforms in the history of the Earth (e.g., Masse, 1993; Vilas et al., 1993; Hunt and Tucker, 1993a; Funk et al., 1993; Grötsch, 1996; Rosales, 1999; Skelton, 2003a; Hillgärtner et al., 2003; Millán et al., 2007). The Maestrat Basin, which was located in tropical latitudes along the eastern margin of the Iberian plate, was no exception (Vennin and Aurell, 2001; Salas et al., 2005; Tomás, 2007; Tomás et al., 2007; Bover-Arnal et al., 2008a).

The main protagonists of these carbonate environments were rudist bivalves, corals and orbitolinids (e.g., Malchus et al., 1996; Vilas et al., 1995; Masse et al., 1998; Skelton and Masse, 2000; Pittet et al., 2002; Tomás et al., 2008). The aforementioned carbonate-producing communities were probably highly sensitive to physico-chemical changes in the ocean–atmosphere system (e.g., Weissert et al., 1998; Pittet et al., 2002; Wissler et al., 2003; Burla et al., 2008). Therefore, the climatically- and tectonically-driven perturbations that occurred

* Corresponding author.
E-mail address: Telm.Bover@uni-bayreuth.de (T. Bover-Arnal).

0037-0738/$ – see front matter © 2009 Elsevier B.V. All rights reserved.
doi:10.1016/j.sedgeo.2009.05.016

throughout Aptian time conditioned these carbonate factories and resulted in the growth and demise of carbonate settings (e.g., Föllmi et al., 1994; Weissert et al., 1998; Pittet et al., 2002; Hillgärtner et al., 2003; Wissler et al., 2003; Weissert and Erba, 2004; Föllmi et al., 2006; Burla et al., 2008; Skelton et al., 2008a).

One of the most important parameters controlling carbonate-producing organisms and, consequently, carbonate platforms, is the relative fluctuations in sea-level (e.g., Kendall and Schlager, 1981; Strasser et al., 1999; Pittet et al., 2000; Bádenas et al., 2004; Aurell and Bádenas, 2004; Rameil, 2005; Thrana and Talbot, 2006; Pomar and Kendall, 2007; Bover-Arnal et al., 2008b). Relative variations in sea-level are due to tectonic activity and eustasy, and they play a major part in determining the available accommodation space that can be filled, as well as the growth potential of light-dependent carbonate-producers (Sarg, 1988; Pomar, 2001). Although it is widely demonstrated that nutrients, temperature, salinity, CO_2, hydrodynamics and other physico-chemical variables also play a significant role in controlling the evolution of carbonate platforms (e.g., Hallock and Schlager, 1986; Föllmi et al., 1994; Weissert et al., 1998; Pomar, 2001; Pittet et al., 2002; Hillgärtner et al., 2003; Mutti and Hallock, 2003; Pomar and Kendall, 2007), the present study will focus on the effects of relative changes in sea-level.

To this end, a high-resolution characterization of a late Early–Middle Aptian carbonate platform succession from the western Maestrat Basin (E Iberian Chain, Spain) was undertaken. This study involved a sedimentological and geometrical analysis of the lithofacies succession, the recognition of variations in stratal stacking patterns and sequence stratigraphy.

Many Cretaceous centered studies dealing with similar subjects have been published in the last decade (Lehmann et al., 1998; Rosales, 1999; Booler and Tucker, 2002; Drzewiecki and Simo, 2000; Borgomano, 2000; Pittet et al., 2002; Kerans, 2002; Bernaus et al., 2003; Hillgärtner et al., 2003; Bauer et al., 2003; Gréselle and Pittet, 2005; Pomar et al., 2005; Husinec and Jelaska, 2006; Gil et al., 2006; Zagrarni et al., 2008). However, what makes this work noteworthy is the exceptional preservation and exposure of the platform-to-basin transition investigated given that it constitutes a high quality case study, which provides evidence that the four systems tracts of Hunt and Tucker (1992), and the surfaces that separate them, can be well documented not only on seismic lines but also in outcrops.

Carbonate platform margins constitute the best setting to study and estimate relative fluctuations in sea-level (Pomar et al., 2005; Gréselle and Pittet, 2005). This privileged location, with the exception of rimmed margins, normally does not have significant stratigraphic gaps, which are common in more proximal parts of the carbonate platforms, nor undergo sediment starvation, which characterizes basinal environments (Pomar et al., 2005). Moreover, well-exposed transitional settings between platform and basin offer an excellent opportunity to observe the complete architecture of the lithofacies, and thus, the possibility to identify the different building blocks (*sensu* Van Wagoner et al., 1988) that form the sedimentary succession.

This paper seeks to a) investigate the response of a late Early–Middle Aptian carbonate system from the northern Tethyan margin to a forced regression and subsequent rise in relative sea-level; b) show all features at outcrop-scale of a four-systems-tract type of sequence; c) identify the different basic accretional units that build up this carbonate succession; d) put these platform carbonates in a global context in order to establish parallelisms and differences with coeval carbonate systems from other Tethyan localities; e) hypothesize about the mechanism that could have triggered the aforementioned relative sea-level fall, and to f) improve our understanding of the Aptian carbonate systems.

In essence, the model proposed herein constitutes an excellent example of how relative sea-level fluctuations of diverse order control facies and architecture of carbonate platforms, and of how sequence stratigraphy can be an effective tool to analyze them. Furthermore, the detailed analysis of lithofacies, parasequences and architecture, in addition to the Tethyan-wide treatment provided in the discussion could constitute a valuable case study not only for those engaged in sequence stratigraphy but also for those working on carbonate platforms and Aptian sedimentary successions.

2. Geological setting of the study area

The late Early–Middle Aptian carbonate platform succession lies in the eastern part of the Iberian Chain (Spain). These sedimentary units crop out along the Camarillas syncline, between the towns of Miravete de la Sierra, Camarillas, Jorcas and Villarroya de los Pinares (Teruel province) (Fig. 1).

Throughout the Late Jurassic–Early Cretaceous time interval, a rifting event linked to the spreading Atlantic Ocean and to the opening of the Bay of Biscay, divided the northeastern Iberian plate into four strongly subsident basins: the Cameros, Columbrets, South Iberian and Maestrat (Salas et al., 2001, 2005). The area analyzed here was situated in the Galve sub-basin (Salas and Guimerà, 1996), which corresponded to a western peripheral part of the Maestrat Basin in the eastern Iberian Chain (Fig. 1). During the Aptian stage, up to 810 m of continental and epicontinental marine, mixed carbonate–siliciclastic sediments were deposited in the sub-basin (Bover-Arnal et al., submitted for publication). Subsequently, as a result of the convergence between the Iberian and European plates during the Late Cretaceous–Miocene period, the Iberian basins were tectonically inverted, giving rise to the Iberian Chain in the Paleogene (Salas and Casas, 1993; Salas et al., 2001).

In the central part of the Galve sub-basin, where the study area is located (Fig. 1), the Aptian sedimentary succession can be divided into five formations: Morella, Xert, Forcall, Villarroya de los Pinares and Benassal (Canérot et al., 1982; Salas et al., 2001; Bover-Arnal et al., submitted for publication). The outcrops analyzed span the late Early–Middle Aptian time slice, and comprise the marly sediments of the top of the Forcall Formation, the platform carbonates of the Villarroya de los Pinares Formation and the marly deposits and carbonate rocks of the lower part of the Benassal Formation. The age of this succession is based on ammonite and rudist biostratigraphy (Moreno and Bover, 2007; Bover-Arnal et al., submitted for publication) (Fig. 2).

The Aptian sedimentary record of the Galve sub-basin can also be divided into four long-term transgressive–regressive (T–R) sequences (Bover-Arnal et al., submitted for publication). The sediments studied constitute the uppermost part of T–R Sequence II and the whole of T–R Sequence III (Fig. 2).

Three well-preserved carbonate platform successions were analyzed to the northwest of Miravete de la Sierra and northeast of Camarillas (Fig. 1). The area studied in Camarillas is interpreted as the proximal part of the carbonate platform established during the late Early Aptian in the central part of the Galve sub-basin (Villarroya de los Pinares Formation). The outcrops located close to Miravete de la Sierra (El Morrón and Las Mingachas, see Fig. 1) correspond to the more distal part and to the more marginal setting of the aforementioned carbonate platform, respectively. The lack of tectonic overprint and vegetation in the three sections offers an excellent opportunity to carry out a sedimentological, geometrical, architectural, stacking pattern and sequence stratigraphic based analysis.

3. Materials and methods

Four sedimentary logs were measured, and the facies variations, subaerial unconformities and, maximum flooding, transgressive and other key sedimentary surfaces were mapped on panoramic photomosaics of the outcrops. A Laser Scanner ILRIS 3D Optech Inc. equipped with a differential GPS Top Con with a receiver GB 1000 and an antenna PG-A1 was used to measure distances, heights and angles within the carbonate strata.

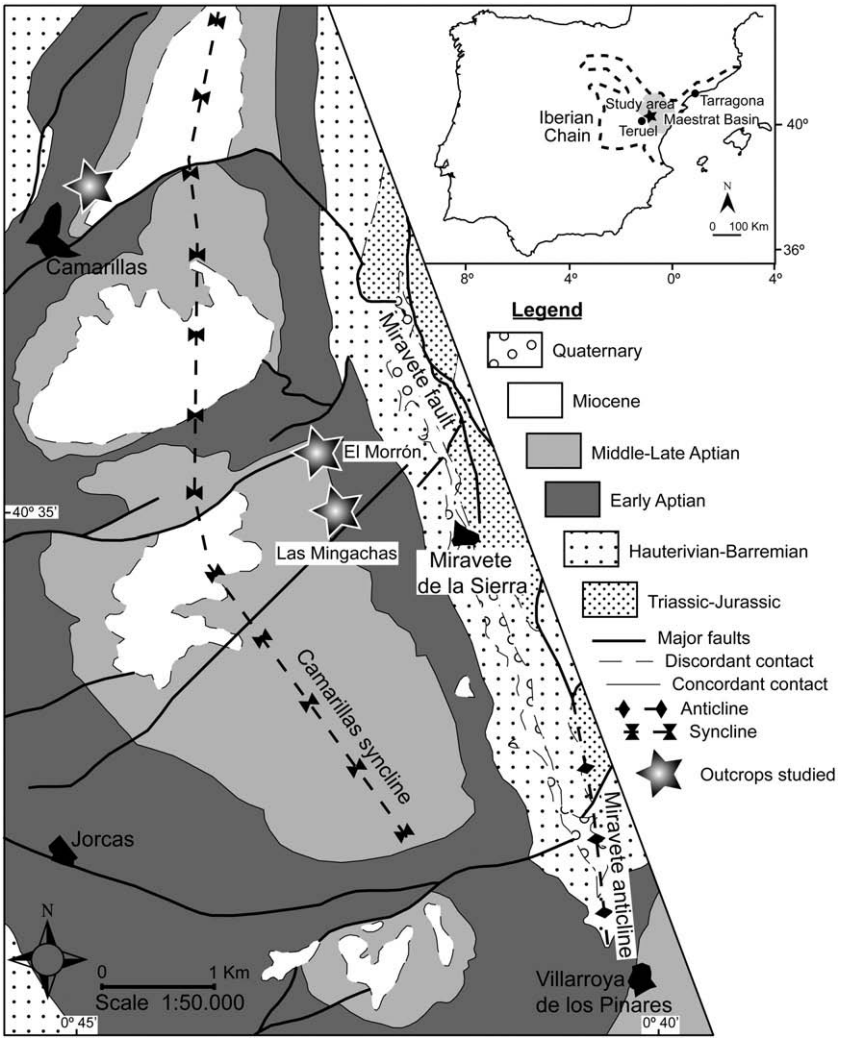

Fig. 1. Geological map of the central Galve sub-basin with its location inside the Iberian Peninsula. The areas studied are marked with a star. Modified after Gautier (1980).

Microfacies analysis was carried out on 82 thin sections. Rock textures follow the classification of Embry and Klovan (1971). The terminology used in the sequence stratigraphic analysis is taken from the works of Hunt and Tucker (1992, 1993b, 1995), Catuneanu (2006) and Catuneanu et al. (2009).

4. Facies Associations and distribution

Ten major lithofacies associations were determined on the basis of lithology, texture, sediment constituents and sedimentary features. These lithofacies assemblages reflect different bathymetric, hydrodynamic and trophic conditions. The recognition of facies heterogeneity and shelf, shelf-margin and slope geometries across the carbonate platform succession permitted to ascribe each facies group to a particular sedimentary setting: platform, slope or basin. The descriptions and interpretations of the lithofacies associations are the following:

4.1. Facies Association I: slightly argillaceous–marly wackestone–packstone

This facies association consists of a few centimeter-thick, light grey, slightly argillaceous–marly limestones with wackestone–packstone texture (Fig. 3A). It exhibits nodular bedding, and at times, occurs interbedded with thin argillaceous–marly levels up to 5-cm-thick. The most characteristic components of this lithofacies are medium- to large-sized discoidal orbitolines (diameter up to 5 mm). Other benthic foraminifera and skeletal fragments of echinoderms, oysters, undiagnosed bivalves and gastropods are also common. Silt- to fine-sand sized quartz grains are commonly present.

This facies association was recognized in platform and slope settings. The presence of argillaceous–marly sediments could be indicative of low hydrodynamic conditions. The input of terrigenous material may have resulted in nutrient-rich episodes, which could have favoured the widespread development of discoidal orbitolinids (Pittet et al., 2002), possibly linked to relatively small-scale transgressive pulses (Vilas et al., 1995).

4.2. Facies Association II: rudist and coral floatstone

Decimeter- to meter-thick (up to 6 m) light grey floatstone limestones dominated by rudists and corals in life position characterize this facies association. The floatstones exhibit massive and tabular bedding. Locally, hardgrounds surmounting the beds and burrow bioturbation are present. The rudist species identified are *Toucasia carinata*, *Polyconites* new species (Skelton et al., 2008b, in press), *Monopleura* sp., *Caprina parvula* and *Offneria* sp. The polyconitid rudists are usually grouped in bouquets. The corals display sheet-like, platy, tabular, branching (Fig. 3B), domal and irregular massive morphologies. *Lithophaga* borings on corals are frequent. Other common constituents of this lithofacies are *Chondrodonta*, oysters, unidentified bivalves, nerineid gastropods, other undiagnosed

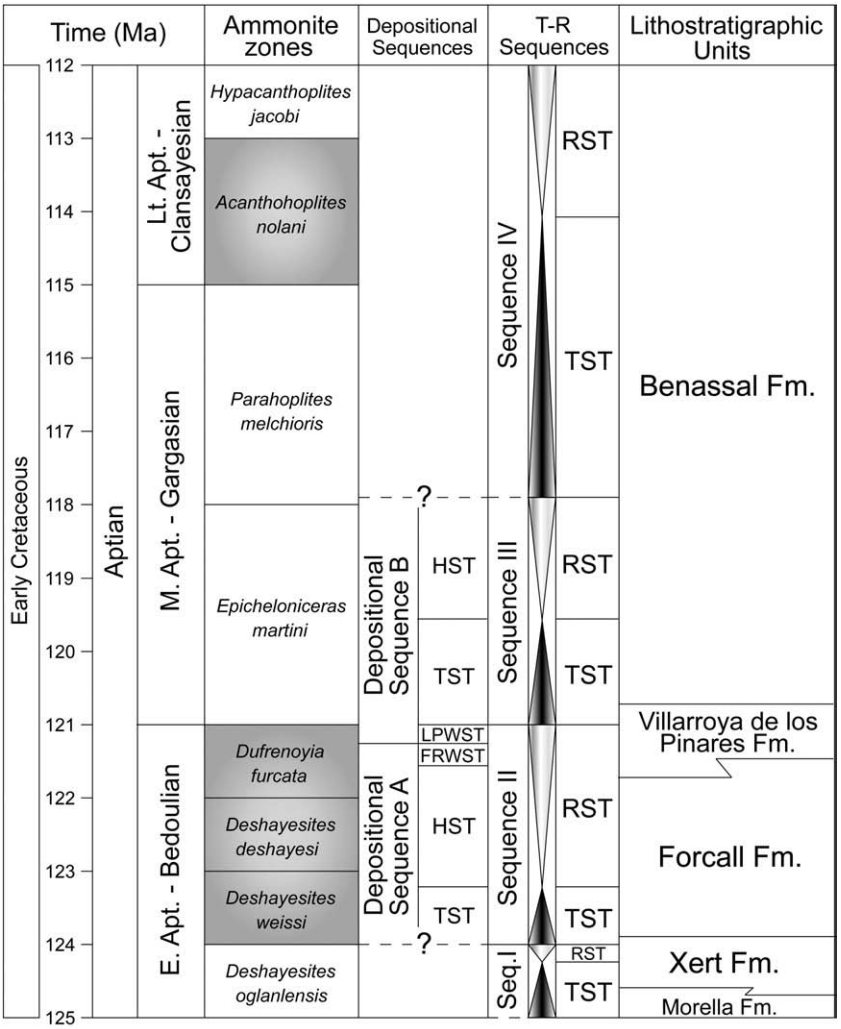

Fig. 2. Aptian lithostratigraphy of the central part of the Galve sub-basin. The ammonite biozones identified are dashed in grey (Moreno and Bover, 2007; Bover-Arnal et al., submitted for publication). Absolute ages are based on Ogg and Ogg (2006).

gastropods, *Orbitolinopsis simplex*, miliolids, other benthic foraminifera, green algae, echinoderms and microencrusters such as sessile foraminifera, *Lithocodium aggregatum*, *Bacinella irregularis* and Peyssonneliaceans encrusting shell debris. Saddle dolomite within coral and rudist skeletal components is common.

Given the large amount of lime mud present and the type of carbonate factory identified, the good fossil preservation and common occurrence in life position suggest that this facies association represents low-energy and muddy platform and platform-margin environments with probable nutrient fluxes as deduced from the strong bioerosion observed on corals (Hallock and Schlager, 1986) and from the broad occurrence of suspension-feeder fauna.

4.3. Facies Association III: rudist and coral reworked floatstone–rudstone

This facies association is characterized by light grey, nodular floatstone–rudstone limestones mainly constituted by fragmented skeletal remains (Fig. 3C). The beds exhibit decimeter- to meter-scale thicknesses (up to 3 m) and display a chaotic structure. The presence of argillaceous–marly drapes within these deposits is conspicuous. The skeletal fragments are generally angular and correspond to the biotic community described in Facies Association II. However, wholly preserved rudists and other molluscs are also commonly found in this facies association.

This lithofacies represents the reworked deposits of Facies Association II and is interpreted as reflecting moderate hydrodynamic conditions in wave-agitated areas of the platform. Nevertheless, these reworked sediments could also be related to storm-induced currents.

4.4. Facies Association IV: peloidal and bioclastic packstone–grainstone

This facies association is formed by light grey packstone–grainstone tabular beds (up to 0.8-m-thick) with plane-parallel and massive stratification. The bases often display erosive surfaces. The limestones with packstone texture are poorly sorted and are largely made up of peloids (diameter up to 0.2 mm), miliolids, other benthic foraminifera and poorly rounded bioclasts of diverse size (up to 4 mm). The bioclasts are mainly skeletal fragments of rudists, echinoderms, corals, green algae, gastropods and other molluscs. The largest bioclasts are commonly bioeroded. The presence of coated grains with a micrite envelope is also worth noting. The limestones with a grainstone fabric are rather well sorted and contain peloids (diameter up to 0.2 mm), orbitolines, miliolids, other benthic foraminifera and poorly rounded bioclasts (size up to 1 mm) of echinoderms, green algae, corals and molluscs. Larger bioeroded skeletal fragments and small entire gastropods are locally present (size up to 3 mm) (Fig. 3D).

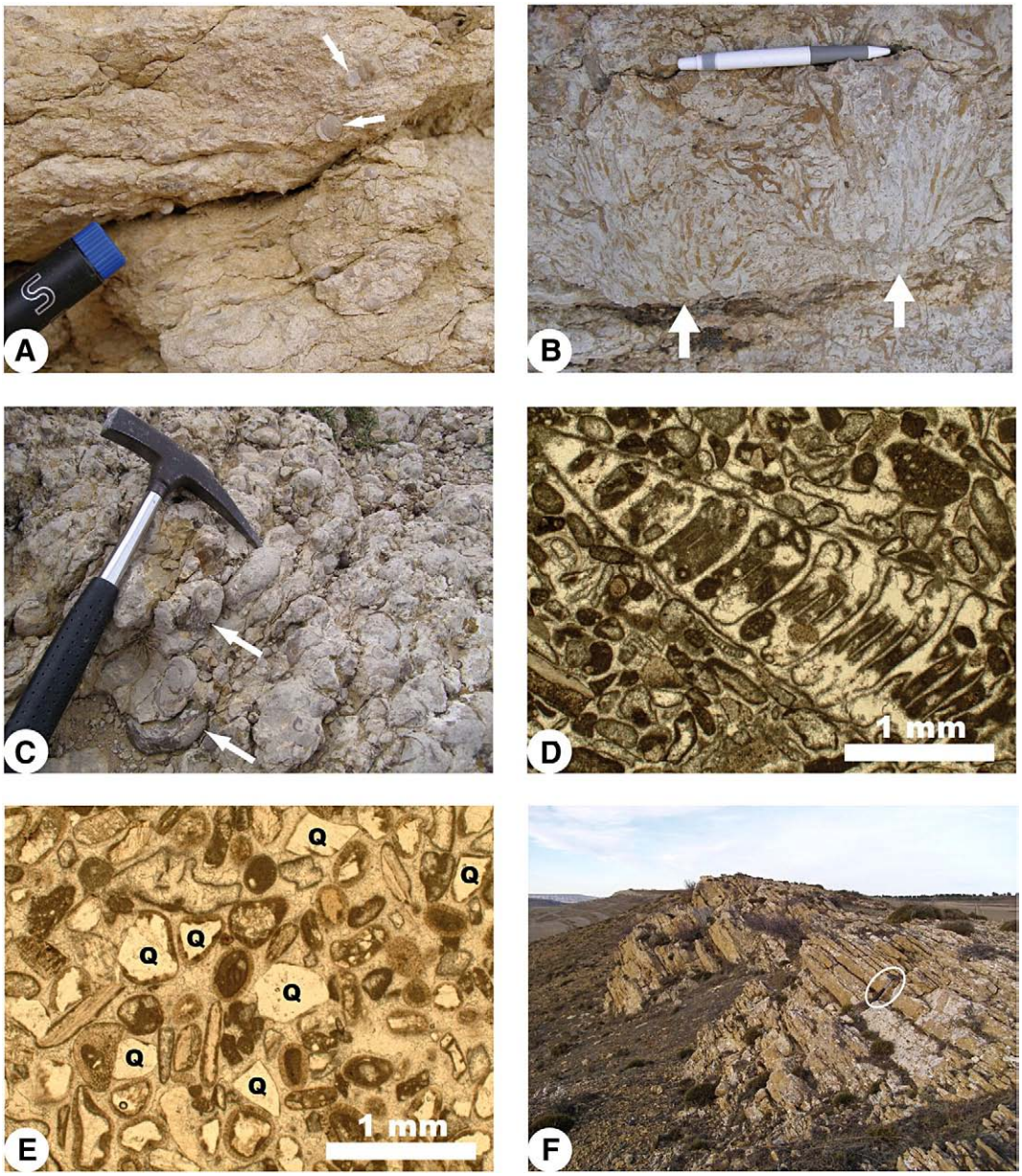

Fig. 3. Sedimentary facies: A) Argillaceous–marly wackestone rich in orbitolines. White arrows point to specimens of Orbitolina. Facies Association I. Las Mingachas (see Fig. 7 for exact location). B) Floatstone of rudists and corals. Note the massive aspect of the lithofacies. White arrows point to delicate branching corals in growth position. Facies Association II. Las Mingachas (see Fig. 7 for exact location). C) Rudist and coral reworked floatstone–rudstone. Note the nodular aspect of the lithofacies. White arrows point to specimens of *Toucasia carinata*. Facies Association III. Camarillas. D) Photomicrograph of peloidal and bioclastic packstone–grainstone microfacies. Note the presence of a small nerineid gastropod at the centre of the image. Facies Association IV. El Morrón. E) Photomicrograph of sandy limestones microfacies. Note the presence of quartz (Q) particles and ooids. Facies Association V. Camarillas. F) Plane-parallel stratified calcarenite rich in oysters. Hammer encircled for scale. Facies Association VI. Camarillas. (For interpretation of the references to colour in this figure legend, the reader is referred to the web version of this article.)

The texture of this lithofacies and the occurrence of plane-parallel stratification suggest that this facies assemblage was deposited in a high-energy environment. The grainstones may reflect an above fair-weather wave-base environment, whereas the packstone textures could represent a slightly deeper-water setting, close to fair-weather wave base.

4.5. Facies Association V: sandy limestones

Decimeter- to meter-thick (up to 6 m), light grey to ochre, fairly well sorted sandy limestones exhibiting cross-bedding and plane-parallel stratification represent this group of lithofacies (Fig. 3E). Locally, the beds of this facies association display erosive and irregular bases. These terrigenous-influenced deposits have a grainstone texture and are composed of angular to sub-rounded, very fine- to medium-grained quartz particles, well rounded ooids of diameter 0.2–0.3 mm with detrital, peloidal and bioclast cores, peloids (diameter up to 0.3 mm), orbitolines, other benthic foraminifera, and sub-angular- to sub-rounded-shaped fragments of echinoderms and molluscs.

The sedimentary structures as well as the rock texture and the components observed suggest that this facies assemblage was formed in high-energy, siliciclastic-influenced shoal environments in a proximal platform setting.

4.6. Facies Association VI: oyster-rich calcarenite

The facies consists of a cross-bedded and plane-parallel stratified orange calcarenite (up to 15-m-thick), rich in oysters (Fig. 3F). This deposit is stacked in a retrograding pattern, and shows a lower part characterized by a well-sorted grainstone fabric, whereas the upper

part is dominated by a poorly- to moderately-sorted packstone–grainstone fabric. The base of this lithofacies is erosive and exhibits clay drapes and mud pebbles, which contain preferentially imbricated silt-sized quartz grains. The main components of the facies are peloids, benthic foraminifera, and fragments of undiagnostic oysters, other unidentifiable molluscs and echinoderms. The bioclasts exhibit sub-rounded to rounded edges. Silt- to fine sand-sized quartz grains are also present. The top of the calcarenite is capped by a hardground displaying borings and ferruginous stains.

The rock texture and the presence of cross-bedding and plane-parallel stratification suggest that this facies association represents a high-energy, shallow platform environment, above or close to fair-weather wave base. The retrograding stacking pattern may reflect a transgressive context.

4.7. Facies Association VII: corals embedded in marls

This assemblage is characterized by small patch-reefs and isolated coral colonies embedded in marls. The corals occur in growth position, showing excellent preservation, with domal (Fig. 4A), irregular massive and branching morphologies. The size of coral colonies ranges from centimeters to meters (up to 2.3-m-width). Coral rubble and dislodged colonies were not observed. *Lithophaga* borings on corals are abundant. The presence of *Polyconites* new species (Skelton et al., 2008b, in press) grouped in bouquets, *Chondrodonta*, oysters, nerineid gastropods, unidentified molluscs, brachiopods, echinoderms, *Dufrenoyia dufrenoyi* and hydrozoans is also typical of this facies association.

This group of lithofacies is characteristic of marly slope environments. The presence of marls with well-preserved sparsely distributed

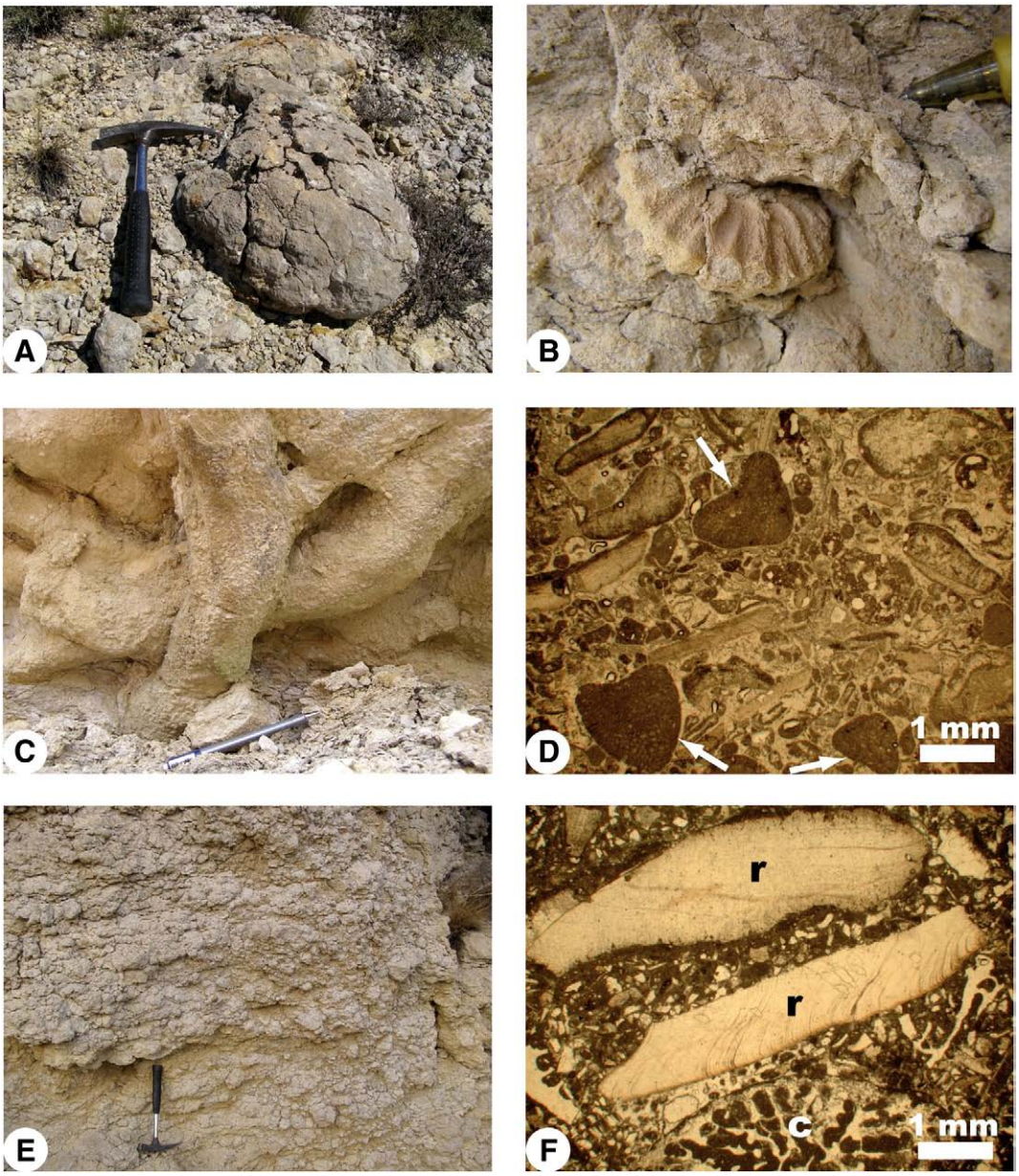

Fig. 4. Sedimentary facies (see Fig. 7 for exact location): A) Flattened dome-shaped coral colony embedded in marls. Facies Association VII. Las Mingachas. B) *Dufrenoyia dufrenoyi* ammonite specimen. Facies Association VIII. Las Mingachas. C) Large *Thalassinoides* bioturbation at the base of a storm-induced turbidite. Note the marly sediments at the lower part of the photograph. Facies Association VIII. Las Mingachas. D) Photomicrograph of the slightly cross-bedded calcarenite wedge microfacies. White arrows point to specimens of *Orbitolinopsis simplex*. Facies Association IX. Las Mingachas. E) Outcrop photograph of the debris-flow deposits. Note the nodular and chaotic aspect of the lithofacies. Facies Association X. Las Mingachas. F) Photomicrograph of debris-flow microfacies. Note the presence of rudist (r) and coral (c) fragments. Facies Association X. Las Mingachas. (For interpretation of the references to colour in this figure legend, the reader is referred to the web version of this article.)

isolated coral colonies, which locally form small patch-reefs, may reflect low hydrodynamic settings, probably, below storm wave-base. Moreover, the occurrence of strong bioerosion on corals and suspension-feeder fauna could be indicative of nutrient-rich conditions.

4.8. Facies Association VIII: marls with interbedded storm-induced turbidites

This facies association basically consists of green marls with interbedded storm-induced deposits and mudstone to wackestone limestones. The marls contain abundant *Palorbitolina lenticularis* and *Praeorbitolina cormyi*, *Dufrenoyia dufrenoyi* (Fig. 4B), undiagnostic oysters, other bivalves, gastropods, unidentified molluscs, brachiopods, echinoderms and pyritized skeletal fragments. Calcareous nodules and bioturbation are also common. The turbidites are characterized by yellowish centimeter- to meter-thick calcarenitic layers with massive stratification and erosive and smooth bases. Locally, the bases of these storm-induced deposits exhibit large *Thalassinoides* burrows (Fig. 4C). The mudstone to wackestone limestones display centimeter- to decimeter-thick massive and nodular stratified yellowish and greyish beds with smooth bases and common bioturbation. The main constituents of the storm-related sediments and the limestones with mudstone and wackestone fabric are silt- to medium sand-sized quartz grains, peloids, orbitolines, other benthic foraminifera, ammonites, and fragments of echinoderms, oysters, rudists and other unidentified molluscs.

The facies assemblage is interpreted as being deposited in relatively deep basinal environments as suggested by the dominant marl, the interbedded storm-induced deposits, and the faunal content. The storm-induced nature of the turbidites is deduced from the presence of abundant silt- to medium sand-sized quartz, which is interpreted as having been transported from proximal settings to basinal environments by storm-induced turbidity currents.

4.9. Facies Association IX: slightly cross-bedded calcarenite

This facies mainly corresponds to a yellowish, slightly planar cross-bedded centimeter- to meter-thick (up to 4 m) calcarenite wedge. The lower part of this wedge presents a tabular stratified calcarenitic layer overlain by a highly bioturbated calcarenitic unit exhibiting nodular bedding. The bases of these deposits have sharp surfaces that exhibit abundant *Planolites* bioturbation and locally, *Thalassinoides* burrows. The lithofacies displays a poorly to moderately sorted packstone-grainstone texture. The main components are peloids, serpulids, *Orbitolinopsis simplex* (Fig. 4D), other benthic foraminifera, *Dufrenoyia furcata* and sub-rounded to rounded fragments of rudists, oysters, other bivalves, gastropods, unidentified molluscs, echinoderms, corals and green algae.

Owing to the basinal position of this calcarenitic wedge, the presence of entire preserved ammonite specimens and the sedimentary structures observed, the facies association is interpreted as allochthonous debris reworked by bottom currents at the toe-of-slope.

4.10. Facies Association X: debris-flow deposits

This facies consists of centimeter- to meter-thick, light grey, nodular-bedded chaotic floatstones and rudstones of rudist and coral fragments (Fig. 4E). Massive stratified beds are rarely present. This facies assemblage commonly displays channelized bodies and erosive surfaces. Locally, slump scars, hardgrounds and unidentified bioturbation occur. The most important constituents of these lithofacies are the same as those described in facies associations II and IV. The fragmented bioclasts mainly show angular edges. The floatstone–rudstone fabric is very poorly sorted (Fig. 4F).

This type of facies is interpreted as debris-flow deposits of facies associations II and IV. The resedimented lithofacies formed under low- to moderate-energy conditions in slope and basinal environments. These deposits occur across slopes, filling in channels or accumulated in lobes at the toe of the slopes.

5. Facies successions

At outcrop scale, the platform stratal arrangement and distribution of the lithofacies assemblages described above basically form deepening–shallowing small-scale (up to few meters thick) symmetrical cycles. These elementary cycles, which are interpreted as having developed in response to high-frequency, low-amplitude relative sea-level fluctuations, correspond to parasequences (*sensu* Spence and Tucker, 2007). The repetition of these basic accretional units builds up the major part of the sedimentary succession studied. Four types of parasequence can be recognized across the carbonate platform system analyzed (Fig. 5):

5.1. Parasequence A

This parasequence is 2- to 8-m-thick and is bounded by smooth transgressive surfaces. Locally, these surfaces are marked by a hardground. This basic accretional unit characterizes the slope environments and is formed in two high-frequency relative sea-level stages: transgressive and regressive.

The transgressive pulse is represented by a unit of irregular massive and dome-shaped corals embedded in marls (Facies Association VII). The corals occur in growth position forming small patch-reefs or isolated colonies. Locally, the presence of a thin orbitoline-rich layer (Facies Association I) characterizes the basal part of these transgressive deposits. This orbitoline-bloom episode could reflect increased nutrient leaching and supply, linked to a high-frequency sea-level rise (Vilas et al., 1995; Pittet et al., 2002).

The subsequent stillstand and fall in relative sea-level increases hydraulic energy in platform settings producing resedimentation and shedding episodes. These debris-flow deposits, which consist of poorly sorted, nodular floatstones and rudstones of rudist and coral fragments (Facies Association X), crossed the slopes and accumulated in a basinal setting, forming lobe deposits. However, oversteepening of the platform margin and storm events may also have caused resedimentation and basinwards transport of platform material.

5.2. Parasequence B

The thickness of this elementary sequence, which is bounded by sharp and irregular transgressive surfaces, ranges between 4 and 8 m. This parasequence is characteristic of proximal-to-distal platform environments and is interpreted as having developed in three relative sea-level pulses: transgressive, early regressive and late regressive.

The transgressive stage is composed of nodular limestone with rudist and coral fragments and a random floatstone to rudstone texture (Facies Association III). Commonly, these deposits are clayey- and marly-influenced and may contain an orbitolina-dominated basal part. The features of the lithofacies suggest reworking in wave- and tidal-influenced shelf settings and thus are interpreted as transgressive lag deposits. However, these reworked sediments could also correspond to storm-induced deposits.

The early regressive pulse (normal regression) records a platform construction episode characterized by floatstones of rudists and delicate branching corals in life position (Facies Association II). The absence of hydrodynamic structures and the occurrence of organisms in growth position may indicate sedimentation below wave-influence, given that protecting shoals, palaeohighs, reefs or other bioherms were not observed basinwards. Nevertheless, sporadic storm events may have lowered wave-base influence, producing reworking and debris-flow episodes.

A falling sea-level (forced regression) results in a basinwards progradation of the energetic belt. Hence, skeletal and peloidal plane-

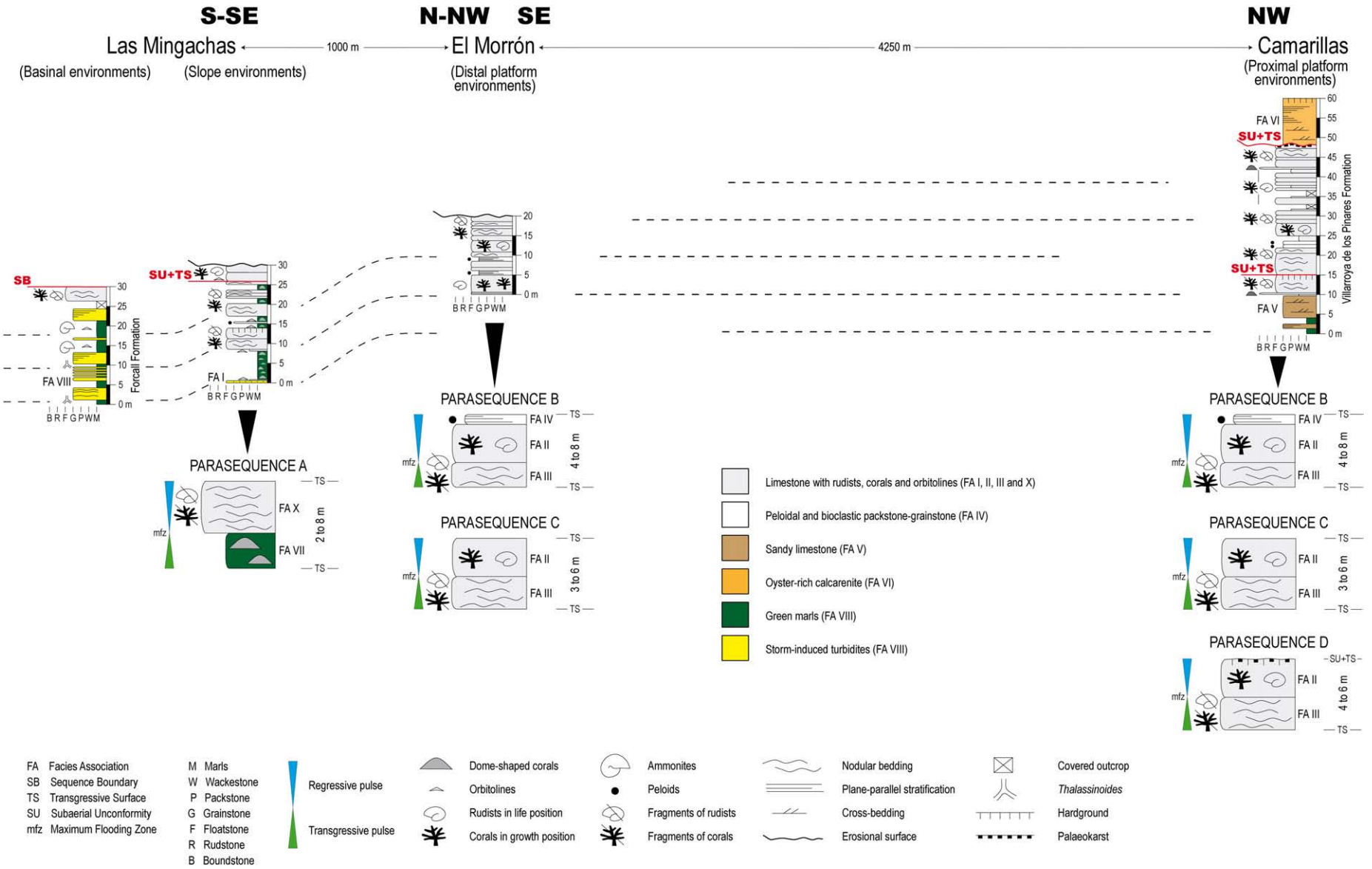

Fig. 5. Simplified scheme of the late Early Aptian platform-to-basin cross-section studied with the measured section logs (see Fig. 1 for location) and the idealized elementary sequences (parasequences) identified within each setting.

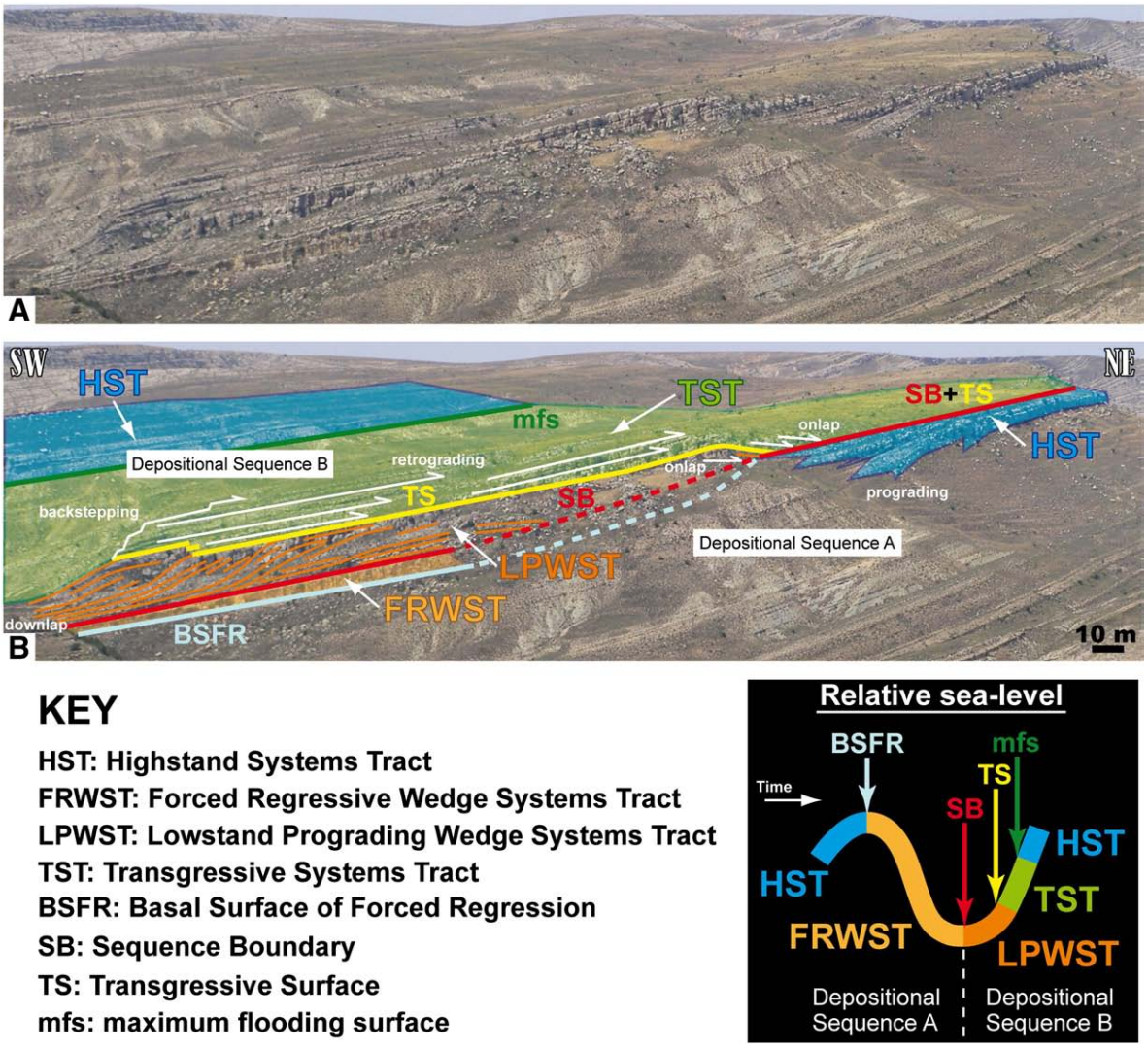

Fig. 6. Photograph of platform-to-basin transition at Las Mingachas (A) (see Fig. 1 for location) with the overall sequence stratigraphic interpretation (B) and the stages of relative sea-level.

parallel stratified limestones with a packstone to grainstone fabric (Facies Association IV) were deposited above the aforementioned deposits of Facies Association II.

5.3. Parasequence C

This type of parasequence is 3- to 6-m-thick and shows the same features described for the parasequence B. However, the most regressive part of the parasequence B, which corresponds to the energetic deposits of Facies Association IV, is not present. The absence of these skeletal and peloidal plane-parallel stratified grainstones and packstones crowning the basic accretional unit could indicate that there was no sediment preservation during the relative sea-level fall (late regressive pulse) or that this forced regressive pulse did not occur or that it was not sufficiently significant to move the energetic belt basinwards.

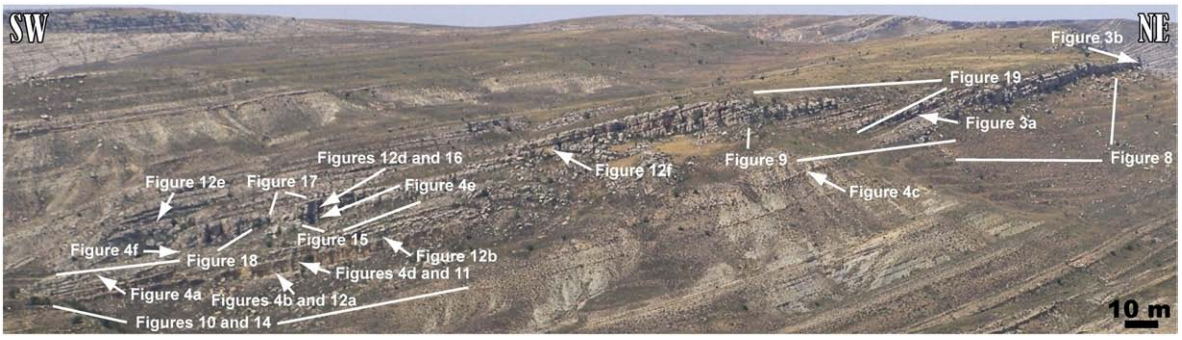

Fig. 7. Photograph of Las Mingachas area (see Fig. 1 for location) displaying the situation of the outcrops and photomicrographs showed in the Figs. 3(a–b), 4 (a–f), 8–12(a–b,d–f), 14–19.

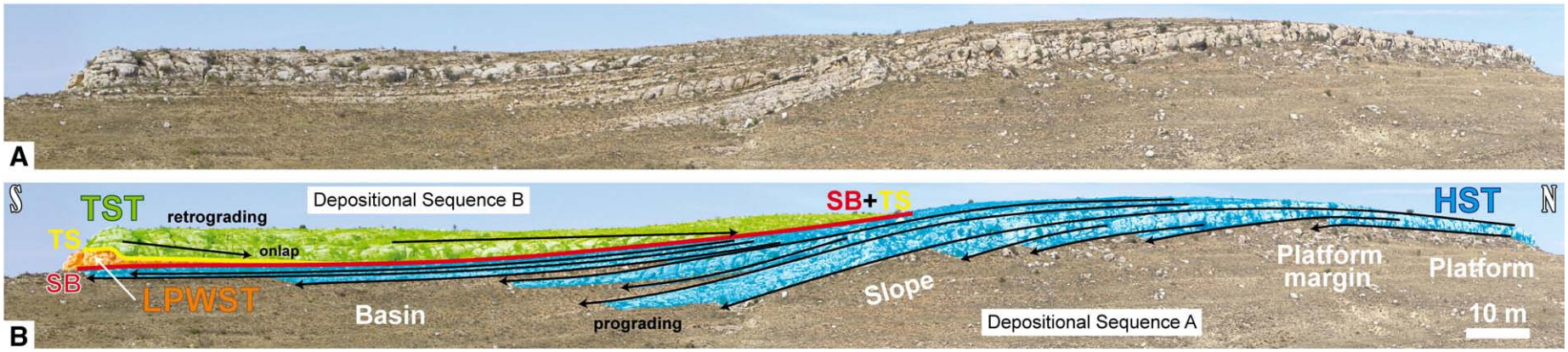

Fig. 8. Photograph of an oblique cross-section from the northeastern part of Las Mingachas (A) (see Fig. 7 for location) showing the sequence stratigraphic interpretation and the shelf-margin geometries, which clearly differentiate the platform, platform-margin, slope and basin depositional settings (B). Note the flat-topped non-rimmed depositional profile that exhibits the carbonate platform. See Fig. 6 for legend.

5.4. Parasequence D

This elementary sequence is typically 4- to 6-m-thick and consists of type C parasequences capped by subaerial exposure surfaces. Locally, these subaerial unconformities correspond to erosive surfaces with a development of palaeokarst. Transgressive surfaces are superimposed on these surfaces affected by subaerial processes, and commonly mask the evidence of subaerial exposure. Hardground development associated with transgressive surfaces is common.

6. Sequence stratigraphic interpretation

In the platform-to-basin transition area of Las Mingachas (Fig. 1), the overall stratal architecture of the facies successions analyzed can be divided into five large-scale differentiated lithostratigraphic units; these reflect longer-term relative sea-level changes and can be interpreted as component systems tracts. These systems tracts occur within two large-scale T–R sequences (Sequence II and III; Fig. 2) described by Bover-Arnal et al. (submitted for publication) in an extensive study of the Aptian evolution of the western Maestrat Basin in the Iberian Chain.

Moreover, the disposition in time and space of these systems tracts seems to be consistent with the model for deposition during base-level fall of Hunt and Tucker (1992, 1993b). Hence, the sequence stratigraphic analysis presented below will be based on the works of these authors. The sedimentary succession analyzed, which embraces T–R sequences II and III, was reinterpreted using depositional sequences in the sense of Van Wagoner et al. (1988). On account of this reinterpretation, two depositional sequences can be construed from the sedimentary record studied: A and B (Fig. 2).

The upper part of Depositional Sequence A, which is of late Early Aptian age (Fig. 2), is composed of Highstand Systems Tract (HST) deposits followed by a Forced Regressive Wedge Systems Tract (FRWST). Depositional Sequence B, which is of uppermost Early Aptian and Middle Aptian age (Fig. 2), is characterized by a Lowstand Prograding Wedge Systems Tract (LPWST) followed by a Transgressive Systems Tract (TST) and the subsequent HST (Fig. 6). All these deposits analyzed show minor tilting towards the SW (Fig. 6).

The locations of the views of the outcrops displayed in the following five headings are shown in Fig. 7.

6.1. Highstand Systems Tract (Depositional Sequence A)

The HST of Depositional Sequence A is distinguished by the development of a large prograding carbonate platform dominated by rudists and corals (Facies Associations II and III), and these essentially conform to the Villarroya de los Pinares Formation. Nevertheless, the presence of high-energy deposits such as sandy limestones (Facies Association V) and skeletal–peloidal packstones and grainstones (Facies Association IV) sedimented throughout this highstand stage is also noteworthy (Fig. 5).

The highstand carbonate shelf extends at least from the north of the town of Camarillas to Las Mingachas (see Fig. 1 for location), where it changes laterally into slope lithofacies (Facies Associations I, VII and X) that pinch out into the basinal marls (Facies Association VIII) of the Forcall Formation (Figs. 5, 6 and 8). At Las Mingachas, the shelf margin exhibits facies heterogeneity and superb platform-to-basin transition geometries (Figs. 6, 8 and 9) that display a flat-topped non-rimmed depositional profile (Fig. 8).

The considerable thicknesses of the beds, the wide diversity and extensive development of facies as well as the carbonate producers observed (see Facies Association II description for species) and the large amount of lime mud, suggest that carbonate production was intense in shelf settings during the HST. The high rate of carbonate accumulation together with the slowing sea-level rise to a near standstill, which is characteristic of a highstand of sea-level, significantly reduced the available accommodation space throughout the late HST. Limited space for vertical accumulation during this late highstand phase is evidenced by type B and C parasequences (Fig. 5) that become thinner upwards in the succession, and by the development of type D parasequences in proximal parts of the carbonate platform (Fig. 5). Moreover, this is also corroborated by the

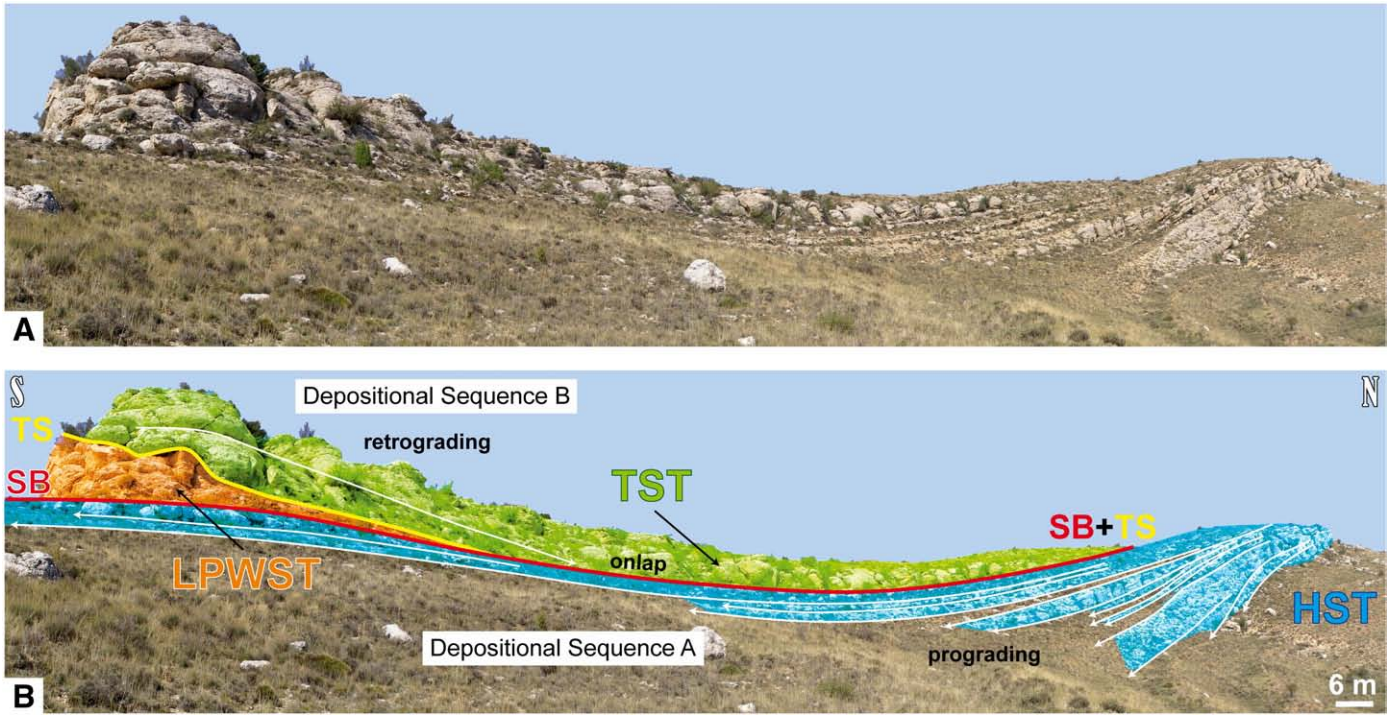

Fig. 9. View from the south of the oblique cross-section located in the northeastern part of Las Mingachas (A) (see Fig. 7 for location) displaying the sequence stratigraphic interpretation (B). See Fig. 6 for legend.

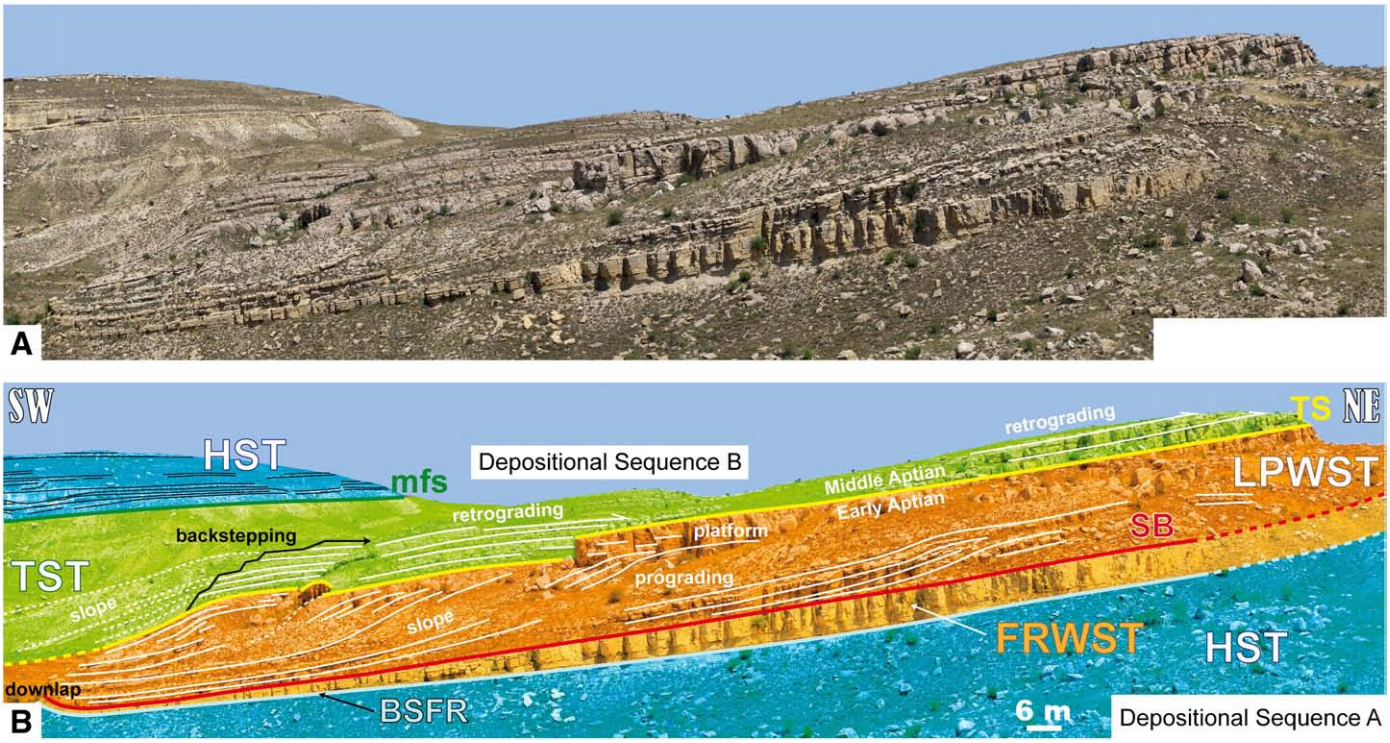

Fig. 10. Photograph of the southern part of Las Mingachas (A) (see Fig. 7 for location) showing the sequence stratigraphic interpretation (B). See Fig. 6 for legend.

overall prograding stacking pattern that exhibits the HST and the episodic downslope dumping of excess sediment (Figs. 6, 8 and 9).

6.2. Forced Regressive Wedge Systems Tract (Depositional Sequence A)

Base-level started to fall with the result that the highstand platform was subaerially exposed, essentially shutting down the carbonate factories and leaving a starved slope. During this relative sea-level drop, the sedimentation of a thick slightly cross-bedded calcarenite wedge (Facies Association IX) occurred basinwards. This calcarenitic wedge corresponds to a detached forced regressive deposit made up of allochthonous debris, which accumulated at the toe of the slope and were reworked by bottom currents. The allochthonous debris resulted from the chemical and mechanical erosion of the subaerially exposed carbonate platform, and the remains of the reduced carbonate-producing community dwelling on the slope. All these sediments deposited in this basinal position during falling relative sea-level are interpreted as the FRWST (Figs. 6 and 10).

The FRWST onlaps the toe of the former highstand slope forming a basin floor component, which is bounded below by the basal surface of forced regression (BSFR) and above by the sequence boundary (SB) (Figs. 6, 10 and 11). The BSFR marks the start of base-level fall at the shoreline, and at Las Mingachas (Fig. 1) it is a sharp surface, which exhibits abundant *Planolites* bioturbation and separates the underlying highstand marls from the first forced regressive calcarenitic unit (Figs. 11 and 12A). Therefore, this surface also corresponds to a drastic change of lithofacies from basinal marls containing abundant orbitolines, ammonites and brachiopods to shallower-water calcarenitic deposits.

The SB indicates the lowest point of relative sea-level (Figs. 6 and 10), and in the area studied it is characterized by a subaerial unconformity, which becomes progressively younger seawards.

Fig. 11. Outcrop photograph of the FRWST (A) (see Fig. 7 for location) displaying the interpreted position of the BSFR and the correlative conformity of the SB (B). Note the sharp contact of these surfaces. See Fig. 6 for legend.

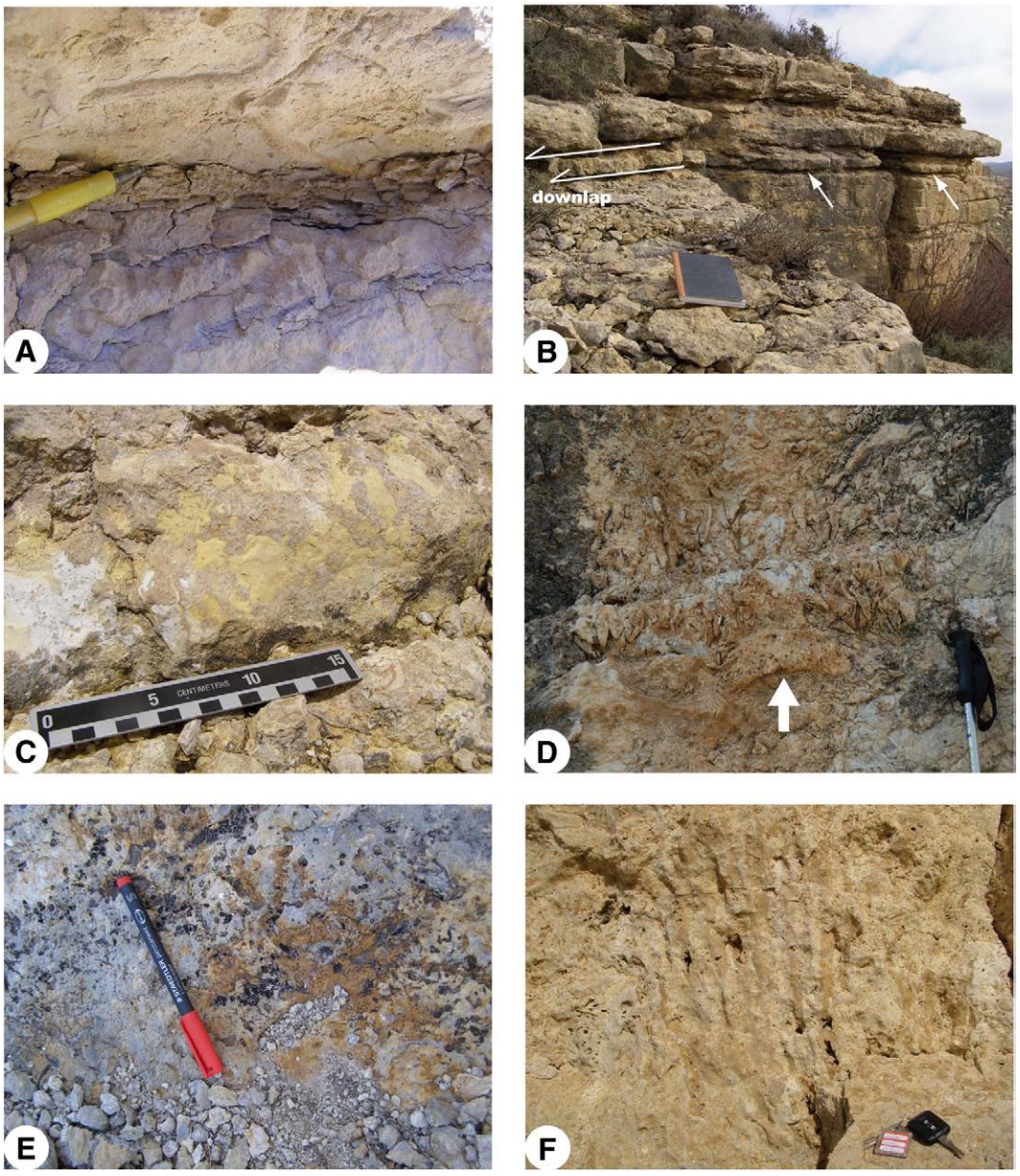

Fig. 12. Sedimentary facies and key sequence stratigraphic surfaces (see Fig. 7 for exact location): A) Detail of the BSFR. Note the sharp contact between the underlying highstand marls and the forced regressive calcarenite, which displays *Planolites* burrows at the base. Las Mingachas. B) Close-up photograph of the correlative conformity surface (SB), which extends above the FRWST and below the LPWST. The notebook lies on this surface, while the white arrows point to it. Note the sharp contact of this surface. Las Mingachas. C) Detail of the surface boundary between the Depositional Sequences A and B displaying palaeokarst development. Camarillas. D) Detail of the lowstand prograding platform lithofacies. Note the *Polyconites* new species rudists (Skelton et al., 2008b, in press) grouped in bouquets. White arrow points to a platy coral. Facies Association II. Las Mingachas. E) Detail of the transgressive surface exhibiting a hardground with a ferruginous crust and borings. Las Mingachas. F) Detail of a rod-like branching coral in growth position in the backsteeping platform (TST). Facies Association II. Las Mingachas. (For interpretation of the references to colour in this figure legend, the reader is referred to the web version of this article.)

Thus, it is reasonable to assume that the highstand platform margin and the uppermost slope situated at Las Mingachas (Fig. 1) were not subaerially exposed for a long time; as a result of this, only a few poorly developed palaeomicrokarst features can be observed. Furthermore, within the uppermost slope and towards the basin, the subaerial unconformity passes to its marine correlative conformity (Fig. 12B), which extends basinwards above the detached forced regressive deposits (FRWST), making its identification difficult (Figs. 6 and 10). Nonetheless, there is clear evidence of subaerial exposure in the proximal parts of the carbonate platform that was established during the HST (Fig. 5) in the vicinity of Camarillas (Fig. 1), where a long-term subaerial exposure surface was developed. This surface exhibits an important truncation related to subaerial processes (Fig. 13) and a broad palaeokarst development (Fig. 12C).

6.3. Lowstand Prograding Wedge Systems Tract (Depositional Sequence B)

With the stillstand and the subsequent rise of relative sea-level, a prograding small carbonate platform of rudists and corals was constructed downslope in the former basin. This platform corresponds to the basal part of Depositional Sequence B and constitutes the LPWST, which is bounded below by the correlative conformity (SB) and above by the transgressive surface (TS) (Figs. 6, 10 and 14). The dip direction of the all-embracing platform system, which developed during this lowstand phase, is around 138° towards the SW.

The lowstand platform architecture displays a flat-topped non-rimmed depositional profile, where shelf lithofacies (Facies Association II) pass into slope deposits (Facies Associations VII and X),

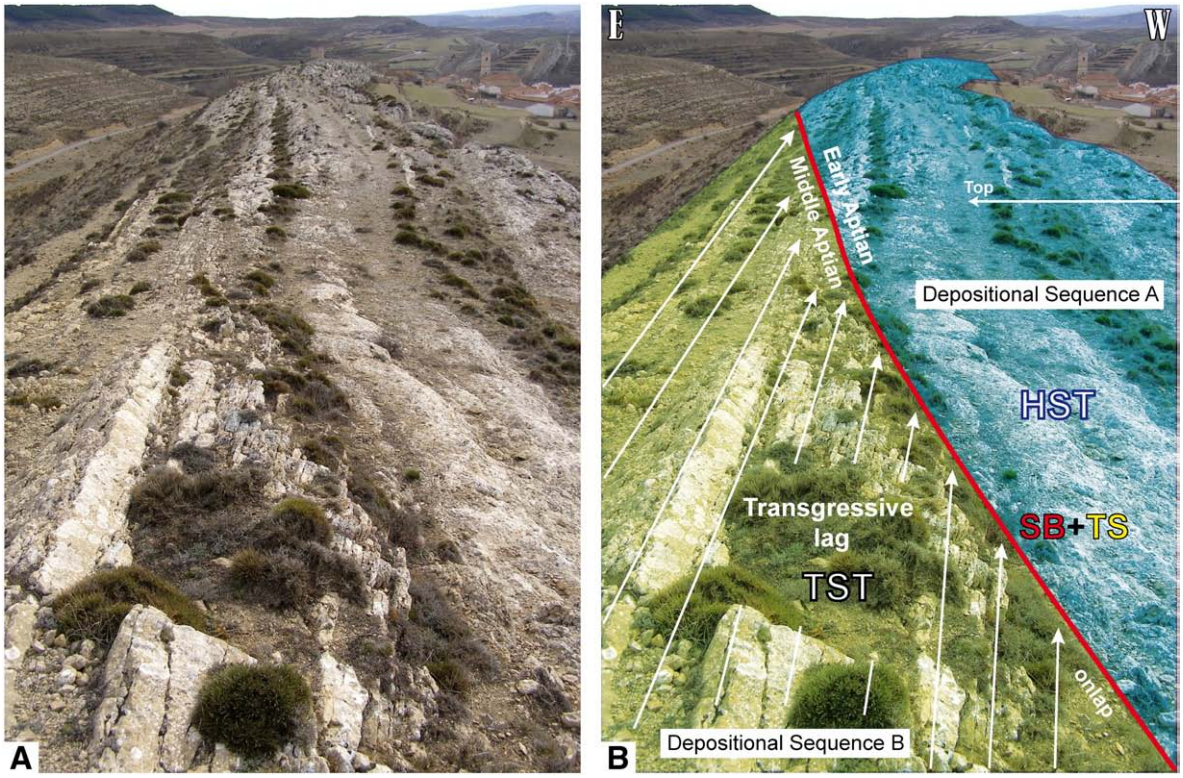

Fig. 13. Photograph of the truncation surface related to subaerial exposure close to the town of Camarillas (A) (see Fig. 1 for location) displaying the sequence stratigraphic interpretation (B). Note how the transgressive lag onlaps the composite surface (SB + TS). Note that the layers are vertical. The town of Camarillas (up-right in the photo) is used for scale. See Fig. 6 for legend.

and then to basinal facies (Facies Associations VIII and X) (Figs. 10 and 15).

The platform facies are massive and show onlapping geometries landwards. Despite the reduced dimensions of the lowstand shelf (Figs. 10 and 15), carbonate production was significant as were shedding episodes. Proliferation of *Polyconites* new species (Skelton et al., 2008b, in press) grouped in bouquets characterizes the shelf margin (Fig. 12D).

The slopes are distinguished by dome-shaped corals embedded in marls (Facies Association VII) with interbedded episodes of nodular-

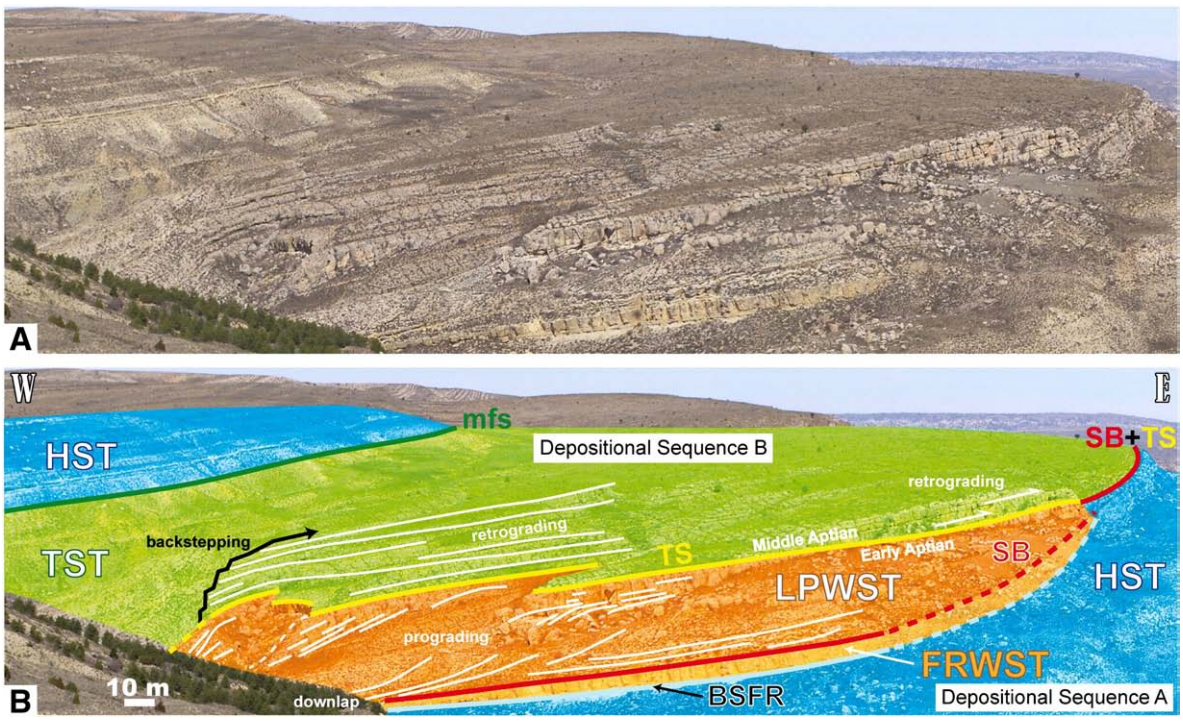

Fig. 14. Panoramic view of the southern part of Las Mingachas (A) (see Fig. 7 for location) showing the sequence stratigraphic interpretation (B). See Fig. 6 for legend.

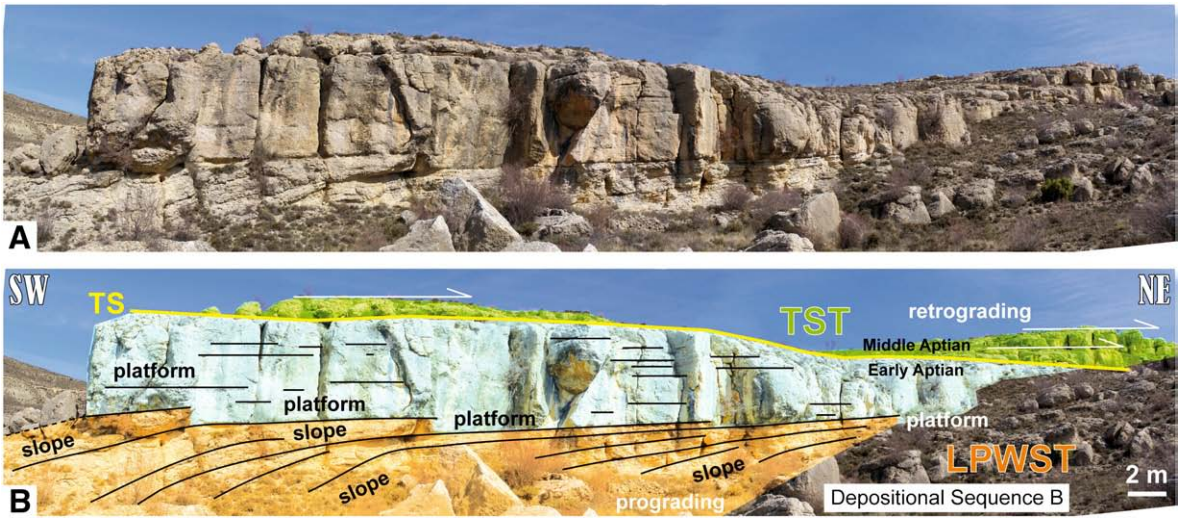

Fig. 15. Outcrop photograph of the lowstand prograding platform (A) (see Fig. 7 for location) displaying the sequence stratigraphic interpretation (B). Note the flat-topped non-rimmed depositional profile that exhibits this carbonate platform and note how it changes laterally from shelf settings to slope environments. The massive lithofacies (above) are construed to be sedimented *in situ*, while the lithofacies with a nodular aspect (below) correspond to resedimented deposits. See Fig. 6 for legend.

shaped debris-flow deposits (Facies Association X) that cross the slopes and downlap over the FRWST (Figs. 6, 10, 14 and 15). Locally, these resedimented slope deposits are channelized or display intraformational smooth and erosive unconformities interpreted as slump scars (Figs. 16 and 17). In this setting, the facies succession is made up of type A parasequences (Fig. 5). The dip angles of these lowstand slopes range between 5 and 25°.

Above the LPWST, the TS marks the end of this stage of normal regression (Figs. 6, 10, 14 and 15). This surface exhibits a sparsely developed hardground with borings and a ferruginous crust (Fig. 12E), and superimposes the SB landwards. Thus, the subaerial unconformity that separates Depositional Sequences A and B becomes a composite sequence boundary (SB + TS) (Figs. 6, 8, 9 and 14).

In addition, the TS may also correspond to the boundary between the Early and the Middle Aptian. In the lowstand carbonate platform of Las Mingachas (Fig. 15), a few specimens of caprinid rudists were identified below the TS, whereas above this surface, this rudist family disappears. According to Skelton (2003b), the disappearance of the rudist family Caprinidae coincides with the Early–Middle Aptian boundary.

Fig. 16. Close-up photograph of the lowstand prograding platform (A) (see Fig. 7 for location) showing a slump scar (B). Note the nodular aspect of these debris-flow deposits. See Fig. 6 for legend.

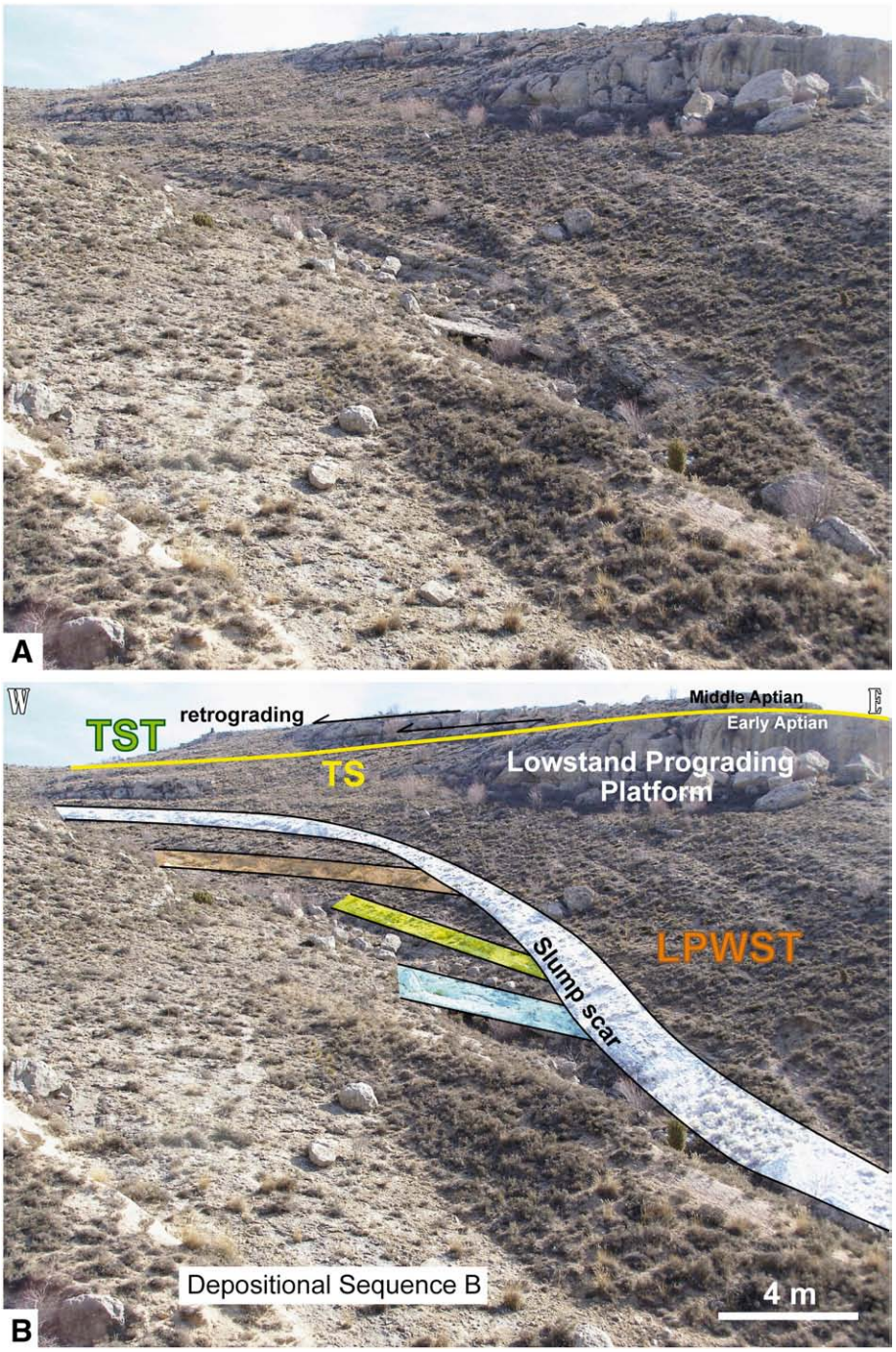

Fig. 17. Outcrop photograph of the lowstand slopes (A) (see Fig. 7 for location) displaying a discordant surface interpreted as a slump scar and the sequence stratigraphic interpretation (B). See Fig. 6 for legend.

6.4. Transgressive Systems Tract (Depositional Sequence B)

During the early TST, the highstand subaerially exposed shelf was progressively flooded towards the land. Sedimentation of a cross-bedded and plane-parallel stratified calcarenite (Facies Association VI), stacked in a retrograding pattern, took place in the Camarillas area (Fig. 1). This high energy deposit onlaps the composite sequence boundary (SB + TS) between Depositional Sequences A and B, and is interpreted as a transgressive lag (Fig. 13). Moreover, this transgressive calcarenite, which can be found despite discontinuities around a kilometric area and is up to 15-m-thick, could be interpreted as a relict of a transgressive migrating barrier island or strand plain.

Seawards, at Las Mingachas (Fig. 1), the transgressive phase started with backstepping of the lowstand platform (Figs. 6, 10 and 18). These platform deposits, also stacked in a retrograding pattern, onlap the composite sequence boundary (SB + TS) landwards (Figs. 6, 8, 9 and 19), and change laterally to marly deposits in a basinwards direction (Figs. 6, 10, 14 and 18).

The backstepping platform facies are essentially characterized by floatstones of rudists and corals in growth position (Fig. 12F) (Facies Association II), as observed for the previous highstand and lowstand platforms. The lithofacies succession that comprises the slope setting of this retrograding platform is basically made up of type A parasequences (Fig. 5). Furthermore, hardgrounds with ferruginous

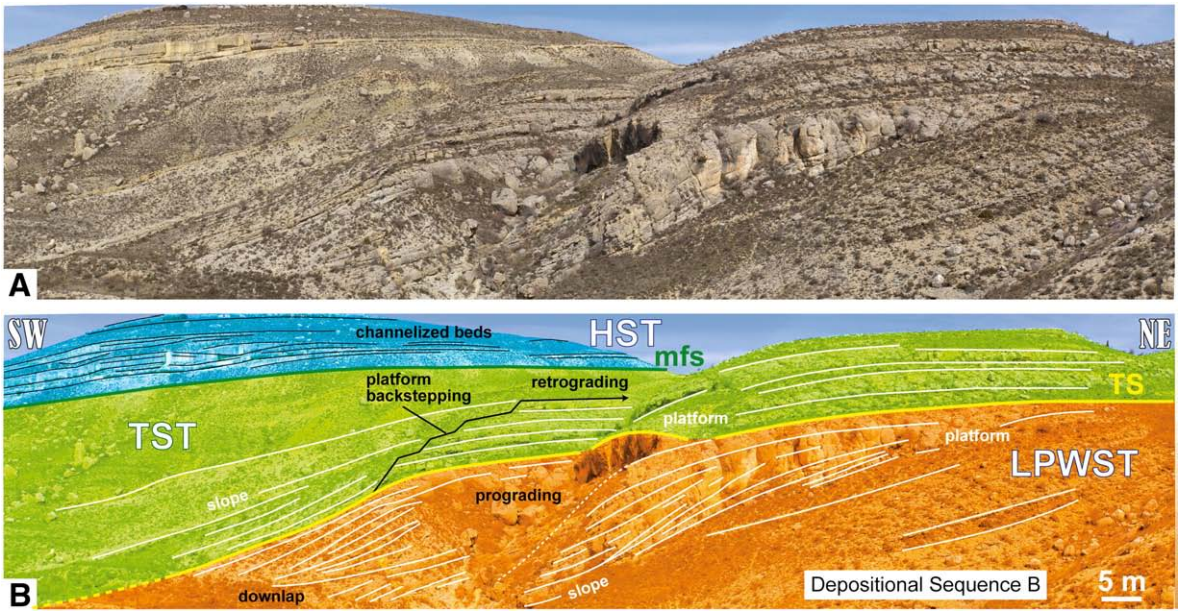

Fig. 18. View of the western part of Las Mingachas (A) (see Fig. 7 for location) showing the platform backstepping geometries and the sequence stratigraphic interpretation (B). See Fig. 6 for legend.

stains, borings and encrusting oysters and corals, are not uncommon in these distal environments of the transgressive platform.

During this period, the carbonate accumulation rate was outpaced by the rate of relative sea-level rise with the result that the retrograding carbonate shelf was finally drowned, evolving into marly sediment upwards in the succession (Figs. 6, 10, 14 and 18). Interbedded highly bioturbated nodular limestones, storm-induced deposits and calcareous nodules containing bivalves, echinoderms

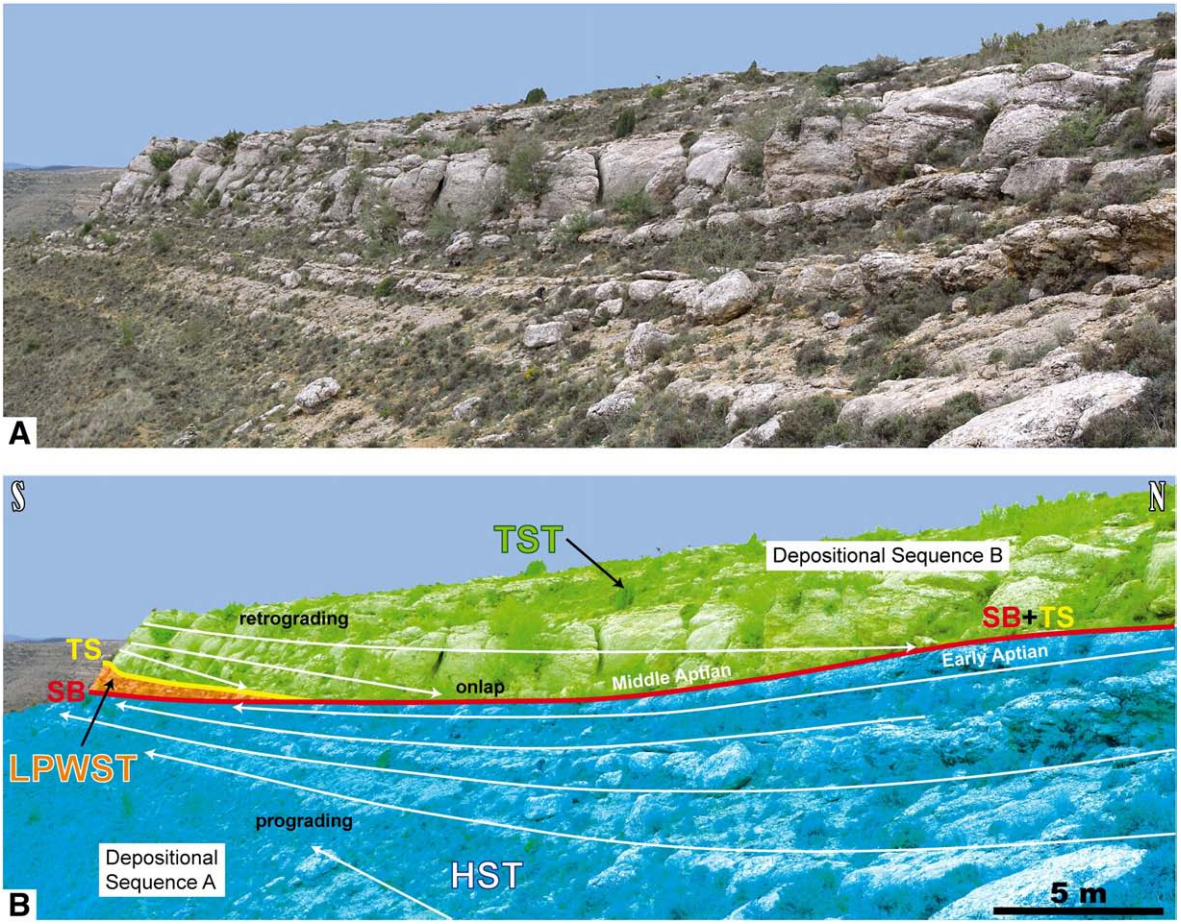

Fig. 19. Outcrop photograph of the northeastern part of Las Mingachas area (A) (see Fig. 7 for location) displaying the transgressive platform onlapping the composite (SB + TS) sequence boundary and the sequence stratigraphic interpretation (B). See Fig. 6 for legend.

and gastropods, also constitute these marly sediments of the upper part of the TST.

The top of the TST is marked by the maximum flooding surface (mfs) of Depositional Sequence B (Figs. 6, 10, 14 and 18). This surface was placed on top of the thickest marl unit that occurs in the transgressive phase, given the absence of sedimentary or biotic features that could reflect the maximum bathymetry reached during this depositional sequence.

6.5. Highstand Systems Tract (Depositional Sequence B)

Above the mfs, the relative sea-level rise progressively slowed to a near sea-level highstand, favouring the development of a new carbonate platform of corals, large rudists and nerineid gastropods (Facies Associations II and III). At Las Mingachas (Fig. 1), the basal highstand marly deposits situated above the mfs rapidly evolve into slope lithofacies represented by the Facies Associations VII and X (Figs. 6, 10, 14 and 18), indicating the presence of carbonate shelves landwards. These slope facies, which consist of marly sediments with domal, irregular-massive and branching corals, interbedded with debris-flow deposits, display a sedimentary succession essentially composed of type A parasequences (Fig. 5). The resedimented shelf materials of Facies Association X show irregular and erosive bases, and mainly occur in the form of channels (Fig. 18).

7. Discussion

The spatial variation of facies and the sequential analysis carried out in the central part of the Galve sub-basin permitted to recognize sequence stratigraphic units of two distinct orders. These units seem to respond to two superposed orders of relative sea-level change, which significantly influenced the carbonate environments that dominated this area during the late Early–Middle Aptian.

Despite the widely held belief that the origin of sea-level fluctuations results from a combination of tectonic and eustatic processes (Vail et al., 1991), high-frequency, short-term relative sea-level variations are commonly interpreted as being essentially controlled by eustasy (Mitchum and Van Wagoner, 1991). These high-frequency sea-level fluctuations, which in the carbonate platform succession analyzed gave rise to deepening–shallowing small-scale cycles (parasequences), are usually interpreted as reflecting global climatic changes linked to orbital forcing within the range of Milankovitch (e.g., Vail et al., 1991; Mitchum and Van Wagoner, 1991; Strasser et al., 1999; Bádenas et al., 2004). Nevertheless, some authors have revealed that, during relative sea-level rise, autocyclic processes such as changes in the sedimentation and/or subsidence rates could also account for these repetitive small-scale sedimentary cycles (Kindler, 1992; Drummond and Wilkinson, 1993). On the other hand, the lower-frequency relative sea-level trends recognized in the area studied, which were interpreted as component systems tracts, can also be attributed, as in the case of the higher-frequency cyclicity, to variations of sea water masses related to allocyclic processes such as changes in climate (Vail et al., 1991). However, in low-frequency, long-term relative sea-level fluctuations, local and regional tectonic activity can also play a decisive role in the accommodation space available, and hence, in the stacking patterns recorded.

In the study area, the systems tracts recognized in the late Early–Middle Aptian time interval occurred during an important subsidence deceleration (Bover-Arnal et al., submitted for publication). Therefore, no signs of vertical movements were identified in the area analyzed for this time interval. Hence, the global eustatic component might have played a more significant role in controlling the HST and FRWST of Depositional Sequence A, and Depositional Sequence B (see Bover-Arnal et al., submitted for publication). In this regard, and despite minor diachronism, the major sea-level fall recorded in the central Galve sub-basin for this period, which caused a forced regression of sea-level in the uppermost late Early Aptian, close to the boundary between the Early and the Middle Aptian, could have had a widespread occurrence along the margin of the Tethys Sea (Sahagian et al., 1996; Hardenbol et al., 1998; Hillgärtner et al., 2003; Gréselle and Pittet, 2005; Husinec and Jelaska, 2006; Yose et al., 2006; Rameil et al. submitted for publication).

The platform margin situated at Las Mingachas (Fig. 1) is the only place in the area studied where the magnitude of this fall in sea-level can be roughly measured. Although the uppermost strata of the late HST of Depositional Sequence A was subaerially exposed and, hence eroded, the height of the top of the preserved highstand deposits with respect to the top of FRWST could be indicative of the order of this sea-level drop. However, the lithofacies of these systems tracts display distinct fossil assemblages, fabrics and sedimentary features, and were probably sedimented in different bathymetries. Therefore, a margin of error of up to several meters should be taken into account. In line with this approximation, the uppermost Early Aptian relative sea-level fall is estimated to be at least 60 m.

The reasons for this global fall in relative sea-level are unknown. Nevertheless, in the central Galve sub-basin, this relative sea-level fall occurred within the *Dufrenoyia furcata* ammonite biozone (Fig. 2; see also Bover-Arnal et al., submitted for publication), which according to Ogg and Ogg (2006) spans 1 My. Assuming this time span for this biozone, and a probable error of hundreds of ky or even a few My, the uppermost Early Aptian relative sea-level fall in the western Maestrat Basin could have had a duration of rather less than 1 My, or at most around 1 My. Thus, one single mechanism or a combination of mechanisms triggering a sea-level fall of at least 60 m at this time would have been necessary to account for this forced regression of relative sea-level.

Immenhauser (2005) and Miller et al. (2005) concluded that probably the most plausible known mechanism that could trigger a global sea-level fall of tens-of-meters per My or less is glacio-eustasy. However, there is contradictory evidence about the feasibility of waxing and waning of ice sheets as the main mechanism governing long-term relative sea-level fluctuations during the Mesozoic (Price, 1999; Immenhauser, 2005; Miller et al., 2005). For this reason, the possibility that this global sea-level fall could have been controlled by a combination of several processes acting at the same time or by mechanisms that could have existed in the past, but have no actual analogues, should not be discarded (Immenhauser, 2005; Miller et al., 2005).

In line with Immenhauser (2005) and Miller et al. (2005), Gréselle and Pittet (2005) in a study of a coetaneous carbonate system from Oman suggested glacio-eustasy as the most likely mechanism that could best explain this widespread forced regression of relative sea-level and other Late Aptian, and Albian major sea-level changes. Peropadre et al. (2008) in a different interpretation of the same outcrops studied here, and following Gréselle and Pittet (2005) and Steuber et al. (2005), already proposed changes in continental ice volumes as a possible explanation for the Aptian sea-level variations that they observed. Thus, given this hypothesis, this sea-level fall that occurred close to the boundary between the Early and Middle Aptian might have been linked to the late Early Aptian cooling episode proposed by Hochuli et al. (1999) and Steuber et al. (2005), which might have increased ice volumes on continents triggering the aforementioned rapid and widespread lowering sea-level.

During this major fall in sea-level, the highstand carbonate system that is basically dominated by rudists and corals of Depositional Sequence A was not able to shift downslope in response to the sea-level fall. Hence, the carbonate factories were essentially shut down throughout the FRWST. Later, with the stillstand and the subsequent rise in relative sea-level, carbonate production was able to recover in the basinal setting, at the toe of the former slope, where a small lowstand prograding platform of rudists and corals developed,

downlapping onto the forced regressive deposits. This differs somewhat from the observations carried out, for the same time interval, in the carbonate systems of Oman (Hillgärtner et al., 2003) and the United Arab Emirates (Yose et al., 2006), where it seems that the carbonate producers displayed enough growth potential to shift downslope during this fall in relative sea-level. This differential response suggests that the sea-level fall was probably too rapid and linear to permit the carbonate-producing organisms to move basinwards in the central part of the Galve sub-basin. On the other hand, in Oman, the widespread sea-level fall could have had a stepped nature or been slower, allowing the carbonate system to shift downslope. Other reasons could be that, at Las Mingachas (Fig. 1) the highstand slope of Depositional Sequence A was too steep and so narrow to permit the establishment of a carbonate factory, or that the space available downslope was not sufficient to accommodate carbonate production. It is also possible that a change in the environmental conditions linked to this relative fall in sea-level could account for the closing down of the carbonate factory.

The carbonate platforms developed during the HST of Depositional Sequence A and the LPWST of Depositional Sequence B display platform-margin clinoforms. These geometries provide new insights into the nature of these Aptian carbonate systems from the Maestrat Basin. The platform-to-basin cross-sections observed show progradational clinoforms that draw a flat-topped non-rimmed depositional profile. The absence of a rim in these carbonate platforms does not seem to have been offset by palaeohigh structures or reworked skeletal sand-banks, which could have acted as a protective barrier to these shelves at this time (see also Bover-Arnal et al., submitted for publication). The fact that the platform sediments are mainly made up of floatstones containing entire rudist specimens occurring locally grouped into bouquets, and small and large coral colonies, commonly displaying delicate branching growth types, suggests a sedimentary environment with low hydrodynamic conditions (Facies Association II). The construction of these carbonate shelves below wave-influence could account for the large amount of lime mud preserved in the facies and for the occurrence of these organisms in life position, along with their excellent preservation. Nevertheless, wave activity could have occasionally reached the shelf carbonate production zone, causing reworking and basinwards transport of sediment during times of lowered sea-level linked to episodic storm events or to high-frequency, low-amplitude short-term sea-level rhythms.

The resulting sequence-stratigraphic framework obtained from the outcrops studied (Fig. 1) reflects a carbonate depositional system conditioned by a fall and subsequent rise in relative sea-level. The sedimentary features, the types of bounding surfaces and the succession of the different stratal stacking patterns recognized, show a depositional model that is consistent with the four systems tract sequence stratigraphic scheme of Hunt and Tucker (1992, 1993b).

The key to a successful sequence stratigraphic analysis primarily depends on the identification and correlation of the stratigraphic surfaces that bound the different systems tracts. The subaerial unconformity, the correlative conformity, the transgressive surface, the maximum flooding surface and the basal surface of forced regression constitute the basis of the chronological framework, which is the essence of sequence stratigraphy. These surfaces were recognized and are widely mappable across the platform-to-basin profile that crops out at Las Mingachas (Fig. 6). However, owing to the oblique cross-section displayed by the outcrop, the BSFR and the marine correlative conformity of the SB cannot be characterized in downdip slope settings. The BSFR is only identified in basinal environments and the SB can only be delineated in shelf, shelf-margin, uppermost slope and basinal settings. Furthermore, at Las Mingachas, the BSFR was placed at the conformable sharp surface that constitutes the base of the first forced regressive calcarenitic episode. This surface, which marks the onset of forced regression (Hunt and Tucker, 1992, 1993b, 1995), separates these reworked allochthonous debris of the FRWST from the underlying marls, which are interpreted as basinal highstand deposits.

Even so, the first arrival of allochthonous debris in the basin should not necessarily mark the start of base-level fall at the shoreline, but these detached forced regressive calcarenitic deposits could represent sediments deposited once the carbonate factory was shut down after the start of base-level fall (Catuneanu, 2006). Thus, the BSFR could be somewhere in the underlying marls. In this regard, Hunt and Tucker (1995) recognized the difficulty of identifying this surface because of the lack of characteristic features due to its conformable nature (see also Plint and Nummedal, 2000; Catuneanu, 2006). In line with the foregoing, the surface that constitutes the base of the first calcarenitic wedge developed during forced regression of the shoreline could correspond to a slope onlap surface (Embry, 1995). Even so, there is no conclusive evidence that demonstrates that the surface delineated as the BSFR (Fig. 6) does not indicate the onset of relative sea-level fall. Moreover, the description of this surface by Hunt and Tucker (1995) in such a manner that it constitutes a sharp surface at the base of basinal redeposited sediments is consistent with the observations made in the field (Fig. 11). Hence, in agreement with Hunt and Tucker (1992, 1993b, 1995), the BSFR was placed at the boundary between the first detached forced regressive calcarenitic deposit and the underlying marls.

The position of the SB within the marine setting, which corresponds to the marine correlative conformity of the subaerial unconformity, has also been a subject of debate (see Kolla et al., 1995; Hunt and Tucker, 1995). Hunt and Tucker (1992) placed this boundary above the basin floor component, which comprises all the deposits sedimented at the toe of the slope during falling relative sea-level. Thus, according to Hunt and Tucker (1992) this surface marks the end of base-level fall. On the other hand, Posamentier et al. (1992) placed the SB below these allochthonous debris deposited in the basinal position during forced regression of the shoreline. In this case, the marine correlative conformity marks the start of base-level fall, and would be equivalent to the BSFR of Hunt and Tucker (1992).

In this study the marine correlative conformity part of the SB was placed above the detached forced regressive unit, deposited at the toe of the slope during base-level fall following Hunt and Tucker (1992, 1995), Helland-Hansen and Gjelberg (1994), and Plint and Nummedal (2000). Therefore, the sequence boundary marks the lowest point of relative sea-level over the platform-to-basin cross-section studied and hence the most basinwards extension of the subaerial unconformity.

8. Conclusions

In this case study, the late Early–Middle Aptian carbonate system from the western Maestrat Basin in the Iberian Chain constitutes a good example of how various orders of relative sea-level change control facies and architecture of carbonate platforms. The carbonate succession analyzed was controlled by two orders of relative sea-level change, which therefore stacked these platform carbonates in sequence stratigraphic units of two orders. Four types of parasequence were developed in relation to higher-frequency sea-level rhythms whereas the lower-frequency cyclicity reflects five differentiated systems tracts within two depositional sequences: the Highstand Systems Tract (HST) and Forced Regressive Wedge Systems Tract (FRWST) of Depositional Sequence A; and the Lowstand Prograding Wedge Systems Tract (LPWST), Transgressive Systems Tract (TST) and Highstand Systems Tract (HST) of Depositional Sequence B. It was possible to characterize these systems tracts on account of the identification of their key bounding surfaces, which are broadly identifiable and correlatable throughout the platform-to-basin transition area studied. The key surfaces with a sequence stratigraphic significance recognized are: a basal surface of forced regression, a subaerial unconformity, a marine correlative conformity, a transgressive

surface and a maximum flooding surface. The sedimentary relationships of the different systems tracts within the lower-frequency relative sea-level cycle are in strong agreement with the dynamics of sedimentation during forced regression and lowstand of relative sea-level of Hunt and Tucker (1992, 1993b).

The major sea-level fall recorded during the uppermost Early Aptian in the central Galve sub-basin (western Maestrat Basin), which subaerially exposed the carbonate platform formed during the first HST and resulted in the deposition of the FRWST, is interpreted as one of global significance. This relative sea-level drop, which was of an order of tens-of-meters, and the subsequent base-level rise occurred within the *Dufrenoyia furcata* biozone. Hence, in order to explain this relative sea-level fall, a mechanism or various mechanisms that could trigger a sea-level drop of tens-of-meters in less than 1 My should be considered. Despite the existence of contradictory evidence, glacio-eustasy could be a plausible mechanism to account for this rapid and widespread forced regression of relative sea-level. In line with this hypothesis, these results are in need of a cooling event during the late Early Aptian, and thus could corroborate the cooling episode proposed in the literature for this time slice (Hochuli et al., 1999; Steuber et al., 2005).

The late Early–Middle Aptian carbonate platforms studied display a flat-topped non-rimmed depositional profile. Palaeohigh structures or shoals, which could have acted as a protective barrier to these shelves at this time, were not observed in the platform-to-basin profile analyzed. Thus, the lithofacies association composed of platform floatstones with well-preserved rudist bivalves and corals in life position does not seem to have been formed in a lagoonal environment but may be interpreted as having been essentially built up below wave-influence. This could be of significance for other Aptian platform carbonate successions lacking platform-to-basin geometries, rimmed margins or clear protecting barriers such as reworked skeletal sand-banks or palaeohigh structures. In these cases, care should be taken to ascribe systematically the characteristic floatstone limestones dominated by rudists and corals in growth position in a lagoonal setting. This late Early–Middle Aptian case study shows that this lithofacies may also develop below wave-influence.

Lastly, the most significant implications of this paper lie in the sequence stratigraphy analysis. The resulting analysis demonstrates that the classic four systems tracts and their key bounding surfaces, even those with a conformable nature such as the basal surface of forced regression and the marine correlative conformity, can be successfully characterized not only at seismic-scale but in outcrops as well. In this regard, the late Early–Middle Aptian platform carbonates cropping out in the central Galve sub-basin might serve as a valuable example of how the theoretical model of Hunt and Tucker (1992) could be applied in outcrop-scale carbonate successions. Hence, in the light of our findings it may be concluded that the outcrops studied here would seem to display a classic example of real rocks fitting theoretical models.

Acknowledgements

The authors would like to express their most sincere appreciation to Maurice E. Tucker who kindly reviewed an early version of this manuscript and provided thoughtful and valuable comments during the peer-review process. We are greatly indebted to Adrian Immenhauser, whose accurate and constructive review resulted in a significant improvement of this paper. We are also especially indebted to Octavian Catuneanu who extensively helped with his useful advice. Special thanks are due to Peter W. Skelton and Eulàlia Gili for determining the rudist species. Grateful thanks are extended to Rolf Schroeder who determined the orbitolinid species and to David García-Sellés for field assistance with the Laser Scanner. We wish to thank Luis Pomar for fruitful discussions in the field. Funding was provided by the Project Bi 1074/1-2 of the Deutsche Forschungsgemeinschaft, the I+D+i Research Projects: CGL2005-07445-CO3-01 and CGL2008-04916, the Consolider-Ingenio 2010 Programme, under CSD 2006-0004 "Topo-Iberia", the Grup Consolidat de Recerca "Geologia Sedimentària" (2005SGR-00890), and the Departament d'Universitats, Recerca i Societat de la Informació de la Generalitat de Catalunya i del Fons Social Europeu.

References

Aurell, M., Bádenas, B., 2004. Facies and depositional sequence evolution controlled by high-frequency sea-level changes in a shallow-water carbonate ramp (late Kimmeridgian, NE Spain). Geological Magazine 141, 717–733.

Bádenas, B., Salas, R., Aurell, M., 2004. Three orders of regional sea-level changes control facies and stacking patterns of shallow platform carbonates in the Maestrat Basin (Tithonian–Berriasian, NE Spain). International Journal of Earth Sciences 93, 144–162.

Bauer, J., Kuss, J., Steuber, T., 2003. Sequence architecture and carbonate platform configuration (Late Cenomanian-Santonian), Sinai, Egypt. Sedimentology 50, 387–414.

Bernaus, J.M., Arnaud-Vanneau, A., Caus, E., 2003. Carbonate platform sequence stratigraphy in a rapidly subsiding area: the Late Barremian–Early Aptian of the Organyà basin, Spanish Pyrenees. Sedimentary Geology 159, 177–201.

Booler, J., Tucker, M.E., 2002. Distribution and geometry of facies and early diagenesis: the key to accommodation space variation and sequence stratigraphy: Upper Cretaceous Congost Carbonate platform, Spanish Pyrenees. Sedimentary Geology 146, 226–247.

Borgomano, J.R.F., 2000. The Upper Cretaceous carbonates of the Gargano-Murge region, southern Italy: a model of platform-to-basin transition. The American Association of Petroleum Geologists Bulletin 84, 1561–1588.

Bover-Arnal, T., Moreno-Bedmar, J.A., Salas, R., Bitzer, K., 2008a. Facies architecture of the late Early–Middle Aptian carbonate platform in the western Maestrat basin (Eastern Iberian Chain). Geo-Temas 10, 115–118.

Bover-Arnal, T., Salas, R., Moreno-Bedmar, J.A., Bitzer, K., Skelton, P.W., Gili, E., 2008b. Two orders of sea-level changes controlled facies and architecture of late Early Aptian carbonate platform systems in the Maestrat Basin (eastern Iberian Chain, Spain). In: Kunkel, C., Hahn, S., ten Veen, J., Rameil, N., Immenhauser, A. (Eds.), SDGG, Heft 58 – Abstract Volume – 26th IAS Regional Meeting/SEPM-CES SEDIMENT 2008 - Bochum, p. 60.

Bover-Arnal, T., Moreno-Bedmar, J.A., Salas, R., Skelton, P.W., Bitzer, K., Gili, E., (submitted for publication). Sedimentary evolution of an Aptian syn-rift carbonate system (Maestrat Basin, E Spain): effects of accommodation and environmental changes. Geologica Acta.

Burla, S., Heimhofer, U., Hochuli, P.A., Weissert, H., Skelton, P., 2008. Changes in sedimentary patterns of coastal and deep-sea successions from the North Atlantic (Portugal) linked to Early Cretaceous environmental change. Palaeogeography, Palaeoclimatology, Palaeoecology 257, 38–57.

Canérot, J., Cugny, P., Pardo, G., Salas, R., Villena, J., 1982. Ibérica Central-Maestrazgo. In: García, A. (Ed.), El Cretácico de España. InUniversidad Complutense de Madrid, pp. 273–344.

Catuneanu, O., 2006. Principles of Sequence Stratigraphy. Elsevier, New York. 386 pp.

Catuneanu, O., Abreu, V., Bhattacharya, J.P., Blum, M.D., Dalrymple, R.W., Eriksson, P.G., Fielding, C.R., Fisher, W.L., Galloway, W.E., Gibling, M.R., Giles, K.A., Holbrook, J.M., Jordan, R., Kendall, C.G.St.C., Macurda, B., Martinsen, O.J., Miall, A.D., Neal, J.E., Nummedal, D., Pomar, L., Posamentier, H.W., Pratt, B.R., Sarg, J.F., Shanley, K.W., Steel, R.J., Strasser, A., Tucker, M.E., Winker, C., 2009. Towards the standardization of sequence stratigraphy. Earth-Science Reviews 92, 1–33.

Drummond, C.N., Wilkinson, B.H., 1993. Carbonate cycle stacking patterns and hierarchies of orbitally forced eustatic sealevel change. Journal of Sedimentary Petrology 63, 369–377.

Drzewiecki, P.A., (Toni) Simo, J.A., 2000. Tectonic, eustatic and environmental controls on mid-Cretaceous carbonate platform deposition, south-central Pyrenees, Spain. Sedimentology 47, 471–495.

Embry, A.F., 1995. Sequence boundaries and sequence hierarchies: problems and proposals. In: Steel, R.J., Felt, V.L., Johannesson, E.P., Mathieu, C. (Eds.), Sequence Stratigraphy on the Northwest European Margin, vol. 5. Norwegian Petroleum Society Special Publication, pp. 1–11.

Embry, A.F., Klovan, J.E., 1971. A Late Devonian reef tract on northeastern Banks Island, N.W.T. Bulletin of Canadian Petroleum Geology 19, 730–781.

Föllmi, K.B., Weissert, H., Bisping, M., Funk, H., 1994. Phosphogenesis, carbon-isotope stratigraphy, and carbonate-platform evolution along the Lower Cretaceous northern Tethyan margin. Geological Society of America Bulletin 106, 729–746.

Föllmi, K.B., Godet, A., Bodin, S., Linder, P., 2006. Interactions between environmental change and shallow water carbonate buildup along the northern Tethyan margin and their impact on the Early Cretaceous carbon isotope record. Paleoceanography 21, PA4211. doi:10.1029/2006PA001313.

Funk, H., Föllmi, K.B., Mohr, H., 1993. Evolution of the Tithonian–Aptian carbonate platform along the northern Tethyan margin, eastern Helvetic Alps. In: Toni Simo, J.A., Scott, R.W., Masse, J.P. (Eds.), Cretaceous Carbonate Platforms: The American Association of Petroleum Geologists, Memoir, vol. 56, pp. 387–407.

Gautier, F., 1980. Villarluengo, hoja n° 543. Mapa Geológico de España 1:50.000. 2ª Serie. 1ª Edición, Servicio de Publicaciones, Ministerio de Industria y Energía, Madrid.

Gil, J., García-Hidalgo, J.F., Segura, M., García, A., Carenas, B., 2006. Stratigraphic architecture, palaeogeography and sea-level changes of a third order depositional sequence: the late Turonian-early Coniacian in the northern Iberian Ranges and Central System (Spain). Sedimentary Geology 191, 191–225.

Gréselle, B., Pittet, B., 2005. Fringing carbonate platforms at the Arabian Plate margin in northern Oman during the Late Aptian–Middle Albian: evidence for high-amplitude sea-level changes. Sedimentary Geology 175, 367–390.
Grötsch, J., 1996. Cycle stacking and long-term sea-level history in the Lower Cretaceous (Gavrovo platform, NW Greece). Journal of Sedimentary Research 66, 723–736.
Hallock, P., Schlager, W., 1986. Nutrient excess and the demise of coral reefs and carbonate platforms. Palaios 1, 389–398.
Hardenbol, J., Thierry, J., Farley, M.B., Jacquin, T., de Gracianski, P.C., Vail, P.R., 1998. Mesozoic and Cenozoic sequence chronostratigraphic framework of European basins. In: de Gracianski, P.C., Hardenbol, J., Jacquin, T., Vail, P.R. (Eds.), Mesozoic and Cenozoic Sequence Stratigraphy of European Basins, SEPM Special Publications 60, charts 1–8.
Helland-Hansen, W., Gjelberg, J.G., 1994. Conceptual basis and variability in sequence stratigraphy: a different perspective. Sedimentary Geology 92, 31–52.
Hillgärtner, H., Van Buchem, F.S.P., Gaumet, F., Razin, P., Pittet, B., Grötsch, J., Droste, H., 2003. The Barremian–Aptian evolution of the eastern Arabian carbonate platform margin (northern Oman). Journal of Sedimentary Research 73, 756–773.
Hochuli, P.A., Menegatti, A.P., Weissert, H., Riva, A., Erba, E., Premoli Silva, I., 1999. Episodes of high productivity and cooling in the early Aptian Alpine Tethys. Geology 27, 657–660.
Hunt, D., Tucker, M.E., 1992. Stranded parasequences and the forced regressive wedge systems tract: deposition during base-level fall. Sedimentary Geology 81, 1–9.
Hunt, D., Tucker, M.E., 1993a. The Middle Cretaceous Urgonian platform of Southeastern France. In: Toni Simo, J.A., Scott, R.W., Masse, J.P. (Eds.), Cretaceous Carbonate Platforms: The American Association of Petroleum Geologists, Memoir, vol. 56, pp. 409–453.
Hunt, D., Tucker, M.E., 1993b. Sequence stratigraphy of carbonate shelves with an example from the mid-Cretaceous (Urgonian) of southeast France. In: Posamentier, H.W., Summerhayes, C.P., Haq, B.U., Allen, G.P. (Eds.), Sequence Stratigraphy and Facies Associations: International Association of Sedimentologists, Special Publications, vol. 18, pp. 307–341.
Hunt, D., Tucker, M.E., 1995. Stranded parasequences and the forced regressive wedge systems tract: deposition during base-level fall—reply. Sedimentary Geology 95, 147–160.
Husinec, A., Jelaska, V., 2006. Relative sea-level changes recorded on an isolated carbonate platform: Tithonian to Cenomanian succession, Southern Croatia. Journal of Sedimentary Research 76, 1120–1136.
Immenhauser, A., 2005. High-rate sea-level change during the Mesozoic: new approaches to an old problem. Sedimentary Geology 175, 277–296.
Kendall, C.G.St.C., Schlager, W., 1981. Carbonates and relative changes in sea level. Marine Geology 44, 181–212.
Kerans, C., 2002. Styles of rudist buildup development along the northern Margin of the Maverick Basin, Pecos River Canyon, Southwest Texas. Gulf Coast Association of Geological Societies Transactions 52, 501–516.
Kindler, P., 1992. Coastal response to the Holocene transgression in the Bahamas: episodic sedimentation versus continuous sea-level rise. Sedimentary Geology 80, 319–329.
Kolla, V., Posamentier, H.W., Eichenseer, H., 1995. Stranded parasequences and the forced regressive wedge systems tract: deposition during base-level fall—discussion. Sedimentary Geology 95, 139–145.
Lehmann, C., Osleger, D.A., Montañez, I.P., 1998. Controls on cyclostratigraphy of Lower Cretaceous carbonates and evaporites, Cupido and Coahuila platforms, northeastern Mexico. Journal of Sedimentary Research 68, 1109–1130.
Malchus, N., Pons, J.M., Salas, R., 1996. Rudist distribution in the lower Aptian shallow platform of la Mola de Xert, Eastern Iberian Range, NE Spain. Revista Mexicana de Ciencias Geológicas 12, 224–235.
Masse, J.P., 1993. Valanginian–Early Aptian carbonate platforms from Provence, Southeastern France. In: Toni Simo, J.A., Scott, R.W., Masse, J.P. (Eds.), Cretaceous Carbonate Platforms: The American Association of Petroleum Geologists, Memoir, vol. 56, pp. 363–374.
Masse, J.P., Borgomano, J., Al Maskiry, S., 1998. A platform-to-basin transition for lower Aptian carbonates (Shuaiba Formation) of the northeastern Jebel Akhdar (Sultanate of Oman). Sedimentary Geology 119, 297–309.
Millán, M.I., Fernández-Mendiola, P.A., García-Mondéjar, J., 2007. Pulsos de inundación marina en la terminación de una plataforma carbonatada (Aptiense inferior de Aralar, Cuenca Vasco-Cantábrica). Geogaceta 41, 127–130.
Miller, K.G., Wright, J.D., Browning, J.V., 2005. Visions of ice sheets in a greenhouse world. Marine Geology 217, 215–231.
Mitchum Jr., R.M., Van Wagoner, J.C., 1991. High-frequency sequences and their stacking patterns: sequence-stratigraphic evidence of high-frequency eustatic cycles. Sedimentary Geology 70, 131–160.
Moreno, J.A., Bover, T., 2007. Precisiones sobre la edad, mediante ammonoideos, de la Fm. Margas del Forcall, Aptiense inferior, en la subcuenca de Galve (Teruel, Espanya). In: Braga, J.C., Checa, A., Company, M. (Eds.), XXIII Jornadas de la Sociedad Española de Paleontología (Caravaca de la Cruz, 3–6 de Octubre de 2007), Libro de resúmenes. InInstituto Geológico y Minero de España y Universidad de Granada, Granada, pp. 151–152.
Mutti, M., Hallock, P., 2003. Carbonate systems along nutrient and temperature gradients: some sedimentological and geochemical constraints. International Journal of Earth Sciences 92, 465–475.
Ogg, J.G., Ogg, G., 2006. Updated by James G. Ogg (Purdue University) and Gabi Ogg to: GEOLOGIC TIME SCALE 2004 (Gradstein, F.M., Ogg, J.G., Smith, A.G. et al.; Cambridge University Press).
Peropadre, C., Meléndez, N., Liesa, C.L., 2008. Variaciones del nivel del mar registradas como valles incisos en la Formación Villarroya de los Pinares en la subcuenca de Galve (Teruel, Cordillera Ibérica). Geo-Temas 10, 167–170.
Pittet, B., Strasser, A., Mattioli, E., 2000. Depositional sequences in deep-shelf environments: a response to sea-level changes and shallow-platform carbonate productivity (Oxfordian, Germany and Spain). Journal of Sedimentary Research 70, 392–407.
Pittet, B., Van Buchem, F.S.P., Hillgärtner, H., Razin, P., Grötsch, J., Droste, H., 2002. Ecological succession, palaeoenvironmental change, and depositional sequences of Barremian–Aptian shallow-water carbonates in northern Oman. Sedimentology 49, 555–581.
Plint, A.G., Nummedal, D., 2000. The falling stage systems tract: recognition and importance in sequence stratigraphic analysis. Geological Society, London, Special Publications 172, 1–17.
Pomar, L., 2001. Types of carbonate platforms: a genetic approach. Basin Research 13, 313–334.
Pomar, L., Kendall, C.G.St.C., 2007. Architecture of carbonate platforms: a response to hydrodynamics and evolving ecology. In: Lukasik, J., Simo, A. (Eds.), Controls on Carbonate Platform and Reef Development: SEPM Special Publication, vol. 89, pp. 187–216.
Pomar, L., Gili, E., Obrador, A., Ward, W.C., 2005. Facies architecture and high-resolution sequence stratigraphy of an Upper Cretaceous platform margin succession, southern central Pyrenees, Spain. Sedimentary Geology 175, 339–365.
Posamentier, H.W., Allen, G.P., James, D.P., Tesson, M., 1992. Forced regressions in a sequence stratigraphic framework: concepts, examples, and exploration significance. The American Association of Petroleum Geologists Bulletin 76, 1687–1709.
Price, G.D., 1999. The evidence and implications of polar ice during the Mesozoic. Earth-Science Reviews 48, 183–210.
Rameil, N., 2005. Carbonate sedimentology, sequence stratigraphy, and cyclostratigraphy of the Tithonian in the Swiss and French Jura Mountains. A high-resolution record of changes in sea level and climate. Ph.D. Thesis, Université de Fribourg, Suisse, GeoFocus 13, pp. 246.
Rameil, N., Immenhauser, A., Csoma, A.É., Warrlich, G., submitted for publication. Surfaces with a long history: the Aptian top Shu'aiba Formation unconformity, Sultanate of Oman. Sedimentology.
Rosales, I., 1999. Controls on carbonate-platform evolution on active fault blocks: the Lower Cretaceous Castro Urdiales platform (Aptian-Albian, northern Spain). Journal of Sedimentary Research 69, 447–465.
Sahagian, D., Pinous, O., Olferiev, A., Zakharov, V., 1996. Eustatic curve for the Middle Jurassic–Cretaceous based on Russian platform and Siberian stratigraphy: zonal resolution. The American Association of Petroleum Geologists Bulletin 80, 1433–1458.
Salas, R., Casas, A., 1993. Mesozoic extensional tectonics, stratigraphy, and crustal evolution during the Alpine cycle of the eastern Iberian basin. Tectonophysics 228, 33–55.
Salas, R., Guimerà, J., 1996. Rasgos estructurales principales de la cuenca cretácica inferior del Maestrazgo (Cordillera Ibérica oriental). Geogaceta 20, 1704–1706.
Salas, R., Guimerà, J., Martín-Closas, C., Meléndez, A., Alonso, A., 2001. Evolution of the Mesozoic Central Iberian rift system and its Cainozoic inversion (Iberian Chain). In: Ziegler, P.A., Cavazza, W., Roberston, A.H.F., Crasquin-Soleau, S. (Eds.), Peri-Tethys Memoir 6: Peri-Tethyan Rift/Wrench Basins and Passive Margins: Mémoires du Muséum National d'Histoire Naturelle 186, Paris, pp. 145–186.
Salas, R., Martín-Closas, C., Delclòs, X., Guimerà, J., Caja, M.A., Mas, R., 2005. Factores principales de control de la sedimentación y los cambios bióticos durante el tránsito Jurásico–Cretácico en la Cadena Ibérica. Geogaceta 38, 15–18.
Sarg, J.F., 1988. Carbonate sequence stratigraphy. In: Wilgus, C.K., Hastings, B.S., Kendall, C.G.St.C., Posamentier, H.W., Ross, C.A., Van Wagoner, J.C. (Eds.), Sea Level Changes: An Integrated Approach: SEPM, Special Publication, vol. 42, pp. 155–181.
Skelton, P.W., 2003a. The Cretaceous World. Cambridge University Press, Cambridge. 360 pp.
Skelton, P.W., 2003b. Rudist evolution and extinction — a north African perspective. In: Gili, E., Negra, M., Skelton, P.W. (Eds.), North African Cretaceous Carbonate Platform Systems. NATO Science Series IV. In: Earth and Environmental Sciences, vol. 28. Kluwer Academic Publishers, pp. 215–227.
Skelton, P.W., Masse, J.-P., 2000. Synoptic guide to the Lower Cretaceous rudist bivalves of Arabia. In: Alsharhan, A.S., Scott, R.W. (Eds.), Middle East Models of Jurassic/Cretaceous Carbonate Systems: SEPM, Special Publication, vol. 69, pp. 89–99.
Skelton, P.W., Gili, E., Bover-Arnal, T., Salas, R., Moreno-Bedmar, J.A., Millán, I., Fernández-Mendiola, K., 2008a. Taxonomic turnover and palaeoecological change among Aptian rudists: and Iberian case study. In: Kunkel, C., Hahn, S., ten Veen, J., Rameil, N., Immenhauser, A. (Eds.), SDGG, Heft 58 – Abstract Volume – 26th IAS Regional Meeting/SEPM-CES SEDIMENT 2008 - Bochum, p. 254.
Skelton, P.W., Gili, E., Bover-Arnal, T., Salas, R., Moreno-Bedmar, J.A., 2008b. A new species of *Polyconites* from the uppermost Lower Aptian of Spain. Eighth International Congress on Rudists. Izmir, Turkey, Abstracts, p. 53.
Skelton, P.W., Gili, E., Bover-Arnal, T., Salas, R., Moreno-Bedmar, J.A., in press. A new species of *Polyconites* from the Lower Aptian of Iberia and the early evolution of polyconitid rudists. Turkish Journal of Earth Sciences.
Spence, G.H., Tucker, M.E., 2007. A proposed integrated multi-signature model for peritidal cycles in carbonates. Journal of Sedimentary Research 77, 797–808.
Steuber, T., Rauch, M., Masse, J.-P., Graaf, J., Malkoc, M., 2005. Low-latitude seasonality of Cretaceous temperatures in warm and cold episodes. Nature 437, 1341–1344.
Strasser, A., Pittet, B., Hillgärtner, H., Pasquier, J.-B., 1999. Depositional sequences in shallow carbonate-dominated sedimentary systems: concepts for a high-resolution analysis. Sedimentary Geology 128, 201–221.
Thrana, C., Talbot, M.R., 2006. High-frequency carbonate–siliciclastic cycles in the Miocene of the Lorca Basin (Western Mediterranean, SE Spain). Geologica Acta 4, 343–354.

Tomás, S., 2007. El sistema arrecifal Aptiense inferior del sector suroriental de la cuenca del Maestrat (Cadena Ibérica). Ph.D. Thesis, Universitat de Barcelona, Barcelona, pp. 192.

Tomás, S., Comas Nebot, M., Salas, R., 2007. La plataforma carbonatada Aptiense superior de Benicàssim-Orpesa (Cuenca del Maestrat, Cadena Ibérica): modelo de depósito. Geogaceta 41, 235–238.

Tomás, S., Löser, H., Salas, R., 2008. Low-light and nutrient-rich coral assemblages in an Upper Aptian carbonate platform of the southern Maestrat Basin (Iberian Chain, eastern Spain). Cretaceous Research 29, 509–534.

Vail, P.R., Audemard, F., Bowman, S.A., Eisner, P.N., Perez-Cruz, C., 1991. The stratigraphic signatures of tectonics, eustasy and sedimentology — an overview. In: Einsele, G., Ricken, W., Seilacher, A. (Eds.), Cycles and Events in Stratigraphy. InSpringer-Verlag, Berlin Heidelberg, pp. 617–659.

Van Wagoner, J.C., Posamentier, H.W., Mitchum, R.M., Vail, P.R., Sarg, J.F., Loutit, T.S., Hardenbol, J., 1988. An overview of the fundamentals of sequence stratigraphy and key definitions. In: Wilgus, C.K., Hastings, B.S., Kendall, C.G.St.C., Posamentier, H.W., Ross, C.A., Van Wagoner, J.C. (Eds.), Sea-level changes: an integrated approach: SEPM, Special Publication, vol. 42, pp. 39–45.

Vennin, E., Aurell, M., 2001. Stratigraphie séquentielle de l'Aptien du sous-bassin de Galvé (Province de Teruel, NE de l'Espagne). Bulletin de la Société Géologique de France 172, 397–410.

Vilas, L., Masse, J.-P., Arias, C., 1993. Aptian mixed terrigenous and carbonate platforms from Iberic and Prebetic Regions, Spain. In: Toni Simo, J.A., Scott, R.W., Masse, J.P. (Eds.), Cretaceous Carbonate Platforms: The American Association of Petroleum Geologists, Memoir, vol. 56, pp. 243–253.

Vilas, L., Masse, J.P., Arias, C., 1995. *Orbitolina* episodes in carbonate platform evolution: the early Aptian model from SE Spain. Palaeogeography, Palaeoclimatology, Palaeoecology 119, 35–45.

Weissert, H., Erba, E., 2004. Volcanism, CO_2 and palaeoclimate: a Late Jurassic–Early Cretaceous carbon and oxygen isotope record. Journal of the Geological Society (London) 161, 695–702.

Weissert, H., Lini, A., Föllmi, K.B., Kuhn, O., 1998. Correlation of Early Cretaceous carbon isotope stratigraphy and platform drowning events: a possible link? Palaeogeography, Palaeoclimatology, Palaeoecology 137, 189–203.

Wissler, L., Funk, H., Weissert, H., 2003. Response of Early Cretaceous carbonate platforms to changes in atmospheric carbon dioxide levels. Palaeogeography, Palaeoclimatology, Palaeoecology, 200, 187–205.

Yose, L.A., Ruf, A.S., Strohmenger, C.J., Schuelke, J.S., Gombos, A., Al-Hosani, I., Al-Maskary, S., Bloch, G., Al-Mehairi, Y., Johnson, I.G., 2006. Three-dimensional characterization of a heterogeneous carbonate reservoir, Lower Cretaceous, Abu Dhabi (United Arab Emirates). In: Harris, P.M., Weber, L.J. (Eds.), Giant Hydrocarbon Reservoirs of the World: From Rocks to Reservoir Characterization and Modeling: AAPG Memoir 88/SEPM, Special Publication, pp. 173–212.

Zagrarni, M.F., Negra, M.H., Hanini, A., 2008. Cenomanian–Turonian facies and sequence stratigraphy, Bahloul Formation, Tunisia. Sedimentary Geology 204, 18–35.